Volume 4

Chapter 5

Stratigraphy and Geological Evolution of the Paramillo de Santa Rosa Volcanic Complex and Its Pleistocene to Holocene Eruptive History

https://doi.org/10.32685/pub.esp.38.2019.05
Published online 27 November 2020

Bernardo Alonso PULGARÍN–ALZATE[1*], Mauricio TAMAYO–ALZATE[2], Ana María CORREA–TAMAYO[3], Julián Andrés CEBALLOS–HERNÁNDEZ[4], Yeni Patricia CRUZ–TORO[5], and Ricardo MÉNDEZ–FAJURY[6]

Abstract This chapter focuses on the evolution through time of Paramillo de Santa Rosa Volcanic Complex, providing new information. The stratigraphy and geological map of the Paramillo de Santa Rosa Volcanic Complex in the Colombian Central Cordillera are presented using the concepts of traditional stratigraphy adapted to the needs of the volcanological environment such that lithostratigraphic units, lithosomes, and unconformities are integrated. Combining this information with new geochronological data, the eruptive history is described in two eruptive periods and six epochs interrupted by recurrent flank collapses and their associated debris avalanches and lahars, as well as time intervals characterized by the activation of processes such as erosion, reworking, and glacial reshaping. The volcanic complex has andesitic to dacitic volcanic products of calc–alkaline affinity, typical of a subduction zone along an active continental margin. The Paramillo de Santa Rosa Volcanic Complex comprises two major overlapping stratovolcanoes and the most recent coulée–dome at the summit of the volcano. Geochronological data indicate that the volcanic complex age extends from the Pleistocene. Chronologically, the major edifices correspond to the remnants of a first volcanic edifice called the Pre–Paramillo de Santa Rosa Volcano that dates from the early to the Middle Pleistocene, and the formation and development of a second edifice called Paramillo de Santa Rosa Volcano from the Middle Pleistocene to the Holocene. These volcanoes produced lava flows and pyroclastic deposits, together with debris avalanche and lahar deposits, as posteruptive processes. The maximum expected eruptive events are concentrated and dilute pyroclastic density currents produced at the summit of the volcano, likely, as a result of explosions and collapses of domes. The present study contributes to the knowledge of Quaternary volcanism of active volcanoes in the northern volcanic segment of Colombia, and confirms that the Paramillo de Santa Rosa Volcano is active and should be considered in local volcanic hazard assessment.

Keywords: *calc–alkaline, Central Cordillera, geological mapping, volcanic stratigraphy, active volcanism.*

1 bpulgarin@sgc.gov.co
Servicio Geológico Colombiano
Dirección de Geociencias Básicas
Observatorio Vulcanológico y Sismológico de Popayán
Calle 5B n.° 2–14
Popayán, Cauca, Colombia

2 mtamayo@sgc.gov.co
Servicio Geológico Colombiano
Dirección de Geociencias Básicas
Observatorio Vulcanológico y Sismológico de Manizales
Avenida 12 de octubre n.° 15–47
Manizales, Colombia

3 acorrea@sgc.gov.co
Servicio Geológico Colombiano
Dirección de Geociencias Básicas
Diagonal 53 n.° 34–53
Bogotá, Colombia

4 jaceballos@sgc.gov.co
Servicio Geológico Colombiano
Dirección de Geoamenazas
Observatorio Vulcanológico y Sismológico de Manizales
Avenida 12 de Octubre n.° 15–47
Manizales, Colombia

5 ycruz@sgc.gov.co
Servicio Geológico Colombiano
Dirección de Geociencias Básicas
Diagonal 53 n.° 34–53
Bogotá, Colombia

6 rmendez@sgc.gov.co
Servicio Geológico Colombiano
Dirección de Geoamenazas
Observatorio Vulcanológico y Sismológico de Manizales
Avenida 12 de octubre n.° 15–47
Manizales, Colombia

* Corresponding author

Citation: Pulgarín–Alzate, B.A., Tamayo–Alzate, M., Correa–Tamayo, A.M., Ceballos–Hernández, J.A., Cruz–Toro, Y.P. & Méndez–Fajury, R. 2020. Stratigraphy and geological evolution of the Paramillo de Santa Rosa Volcanic Complex and its Pleistocene to Holocene eruptive history. In: Gómez, J. & Pinilla–Pachon, A.O. (editors), The Geology of Colombia, Volume 4 Quaternary. Servicio Geológico Colombiano, Publicaciones Geológicas Especiales 38, p. 197–226. Bogotá. https://doi.org/10.32685/pub.esp.38.2019.05

Resumen Este capítulo se enfoca en la evolución a través del tiempo del Complejo Volcánico Paramillo de Santa Rosa, y proporciona nueva información. Se presentan la estratigrafía y el mapa geológico del complejo volcánico localizado en la cordillera Central de Colombia a partir del uso de los conceptos tradicionales de estratigrafía adaptados a las necesidades del entorno volcánico donde se integran las unidades litoestratigráficas, los litosomas y las inconformidades. Combinando esta información con nuevos datos geocronológicos, la historia eruptiva de este complejo volcánico se describe en dos períodos eruptivos y seis épocas interrumpidas por colapsos de flanco volcánico recurrentes y sus correspondientes avalanchas de escombros y lahares, así como intervalos de duración variable caracterizados por la activación de procesos erosivos, retrabajamiento y modelado glaciar. El complejo volcánico tiene productos andesíticos a dacíticos de afinidad calcoalcalina, típicos de una zona de subducción en una margen continental activa. El Complejo Volcánico Paramillo de Santa Rosa comprende dos estratovolcanes mayores superpuestos y un domo de lava tipo *coulée* más reciente en la cima del volcán. Los datos radiométricos disponibles indican que la edad de este complejo volcánico se extiende desde el Pleistoceno. Cronológicamente, los edificios mayores corresponden a los restos de un primer edificio volcánico denominado Volcán Pre Paramillo de Santa Rosa que data del Pleistoceno temprano a Medio, y la formación y desarrollo de un segundo edificio llamado Volcán Paramillo de Santa Rosa del Pleistoceno Medio al Holoceno. Estos volcanes produjeron flujos de lava y depósitos piroclásticos, junto con avalanchas de escombros y depósitos de lahar, como procesos poseruptivos. Los máximos eventos eruptivos esperados son la generación de corrientes de densidad piroclástica concentradas y diluidas producidas en la cima del volcán, probablemente asociadas con explosiones y colapsos de domos. Este estudio contribuye al conocimiento del volcanismo cuaternario de volcanes activos en el segmento norte de los volcanes colombianos, y confirma que el Paramillo de Santa Rosa es un volcán activo y debe ser considerado para la evaluación local de la amenaza volcánica.

Palabras clave: *calcoalcalino, cordillera Central, cartografía geológica, estratigrafía volcánica, volcanismo activo.*

1. Introduction

The Paramillo de Santa Rosa Volcanic Complex (PSRVC) is part of the northernmost volcanism in the Central Cordillera of Colombia (Figure 1) that is bounded to the north and south by San Diego and Cerro Machín Volcanoes, respectively, and is linked to an extensional tectonic regime in the N–S and NE–SW directions due to the Romeral and Palestina Fault Systems. It is part of the San Diego–Cerro Machín Volcano–Tectonic Province (Martínez et al., 2014) and Parque Nacional Natural Los Nevados. The most recent edifice, called Paramillo de Santa Rosa Volcano (PSRV), is confirmed as active in a state of repose that has had Holocene eruptions identified in this study, periodic seismic activity, fumaroles, and hot springs. The springs are located mainly to the W of the volcano and, according to Alfaro et al. (2002), may correspond to a geothermal system independent from the Nevado del Ruiz system and probably having a higher reservoir temperature.

The PSRVC is composed of a large variety of volcanic products (lava flows, lava domes, pyroclastic products, lahars, debris avalanche, and epiclastic deposits). Furthermore, the PSRVC is an important source of the Quindío–Risaralda Fan deposits. All the products of PSRVC are andesitic to dacitic with calc–alkaline affinity.

Papers in the literature regarding the PSRVC have mainly focused on geomorphological (Central Hidroeléctrica de Caldas [CHEC], 1983; Herd, 1974; Martínez et al., 2014; Robertson et al., 2002;Thouret, 1988; Thouret et al., 1985), geothermal (Alfaro et al., 2002; Central Hidroeléctrica de Caldas, 1983), structural (Bohórquez et al., 2005; Espinosa, 2000; Central Hidroeléctrica de Caldas, 1983; Guarín, 2008; Lalinde, 2004; Thouret, 1988), and ecological (Kuhry, 1988; Kuhry et al., 1983; Thouret & van der Hammen, 1981) fields, but knowledge of its eruptive history and geological evolution was lacking. For this purpose, the current chapter presents an integrated study on stratigraphy, geochronology, tectonics, geomorphology, petrography, and geochemistry of the PSRVC through the use of lithostratigraphic units, lithosomes, and unconformities, adapting the methodology presented by Lucchi (2013), along with units of volcanic activity according to Fisher & Schmincke (1984). The main periods and epochs of volcanic activity are separated by erosional and non–depositional times of variable duration, volcano–tectonic collapses, and intense episodes of glacial activity.

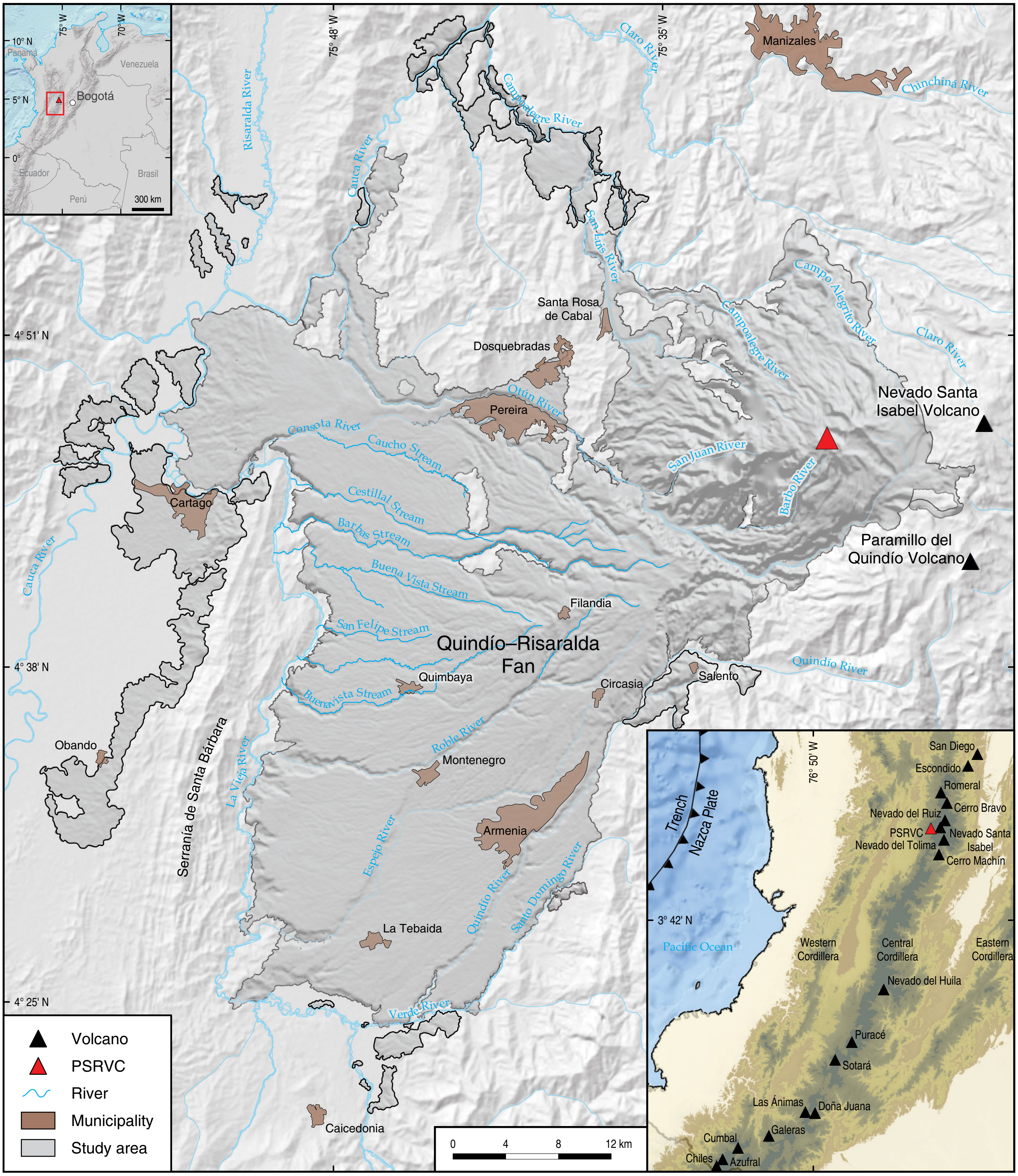

Figure 1. Schematic map showing the location of the PSRVC in the northern volcanic zone of the Central Cordillera of Colombia, together with the main geomorphological features on a shaded relief DEM image.

The geological map of the PSRVC is presented at the proximal (Figure 2a, 2b, 2c, 2d), medial, and distal zones (Figure 3a, 3b) at different scales. Additionally, regional geological information at 1:100 000 and 1:500 000 scales were used (Caballero & Zapata, 1984; Central Hidroeléctrica de Caldas, 1983; Estrada & Viana, 1998; Gómez et al., 2015; González,

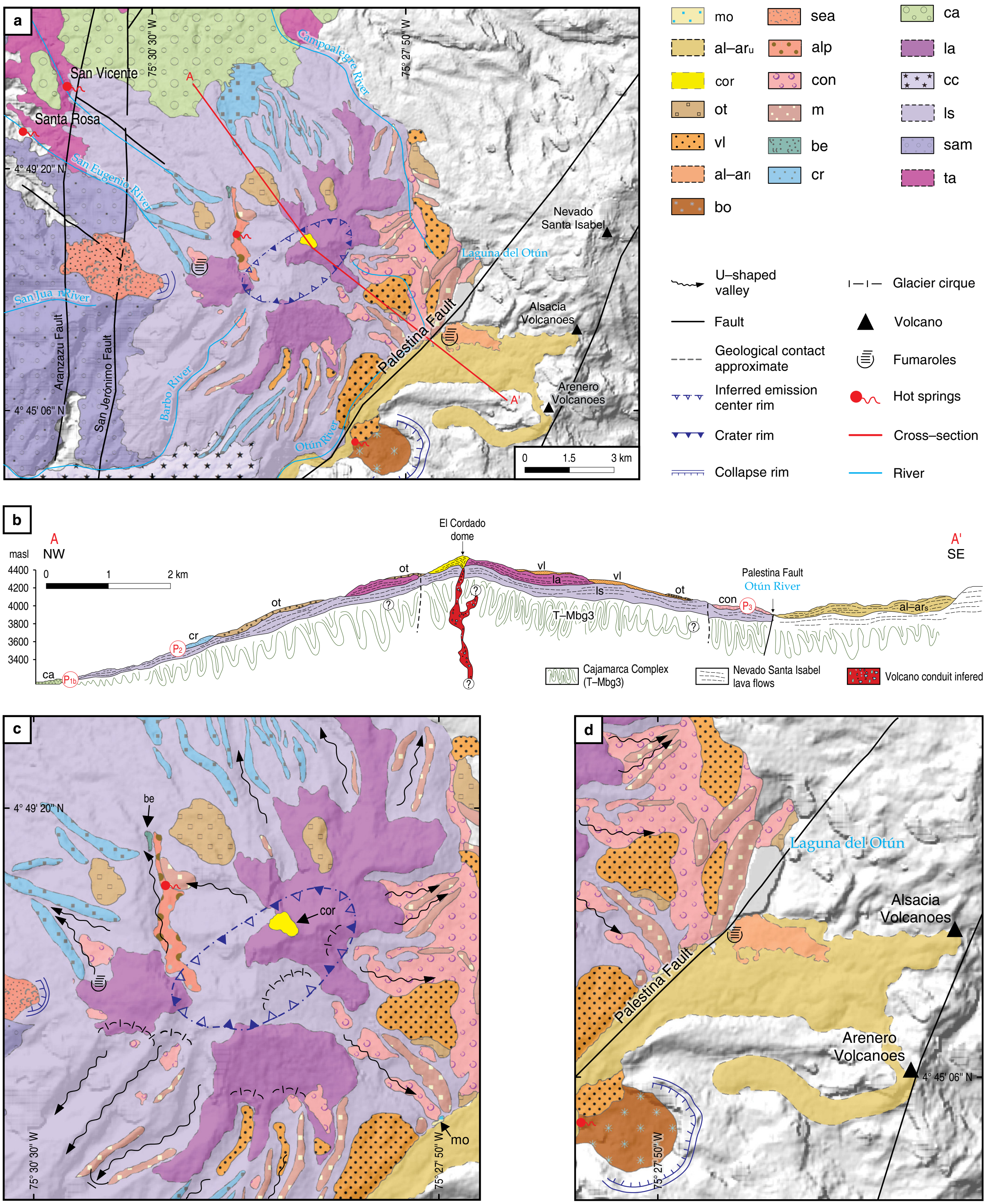

Figure 2. Schematic geological map and cross–section of the PSRVC merged on a shaded relief image of the study area (30 m resolution, NASA). **(a)** Distribution of the lithostratigraphic units recognized in the proximal zone (labels of the stratigraphic succession can be found in Figure 4. The basement is represented by the areas with no colors). **(b)** NW–SE geological cross–section (A–A' in Figure 2a) that includes only deposits of the Paramillo de Santa Rosa lithosome. **(c, d)** Detailed views in the proximal area of PSRVC.

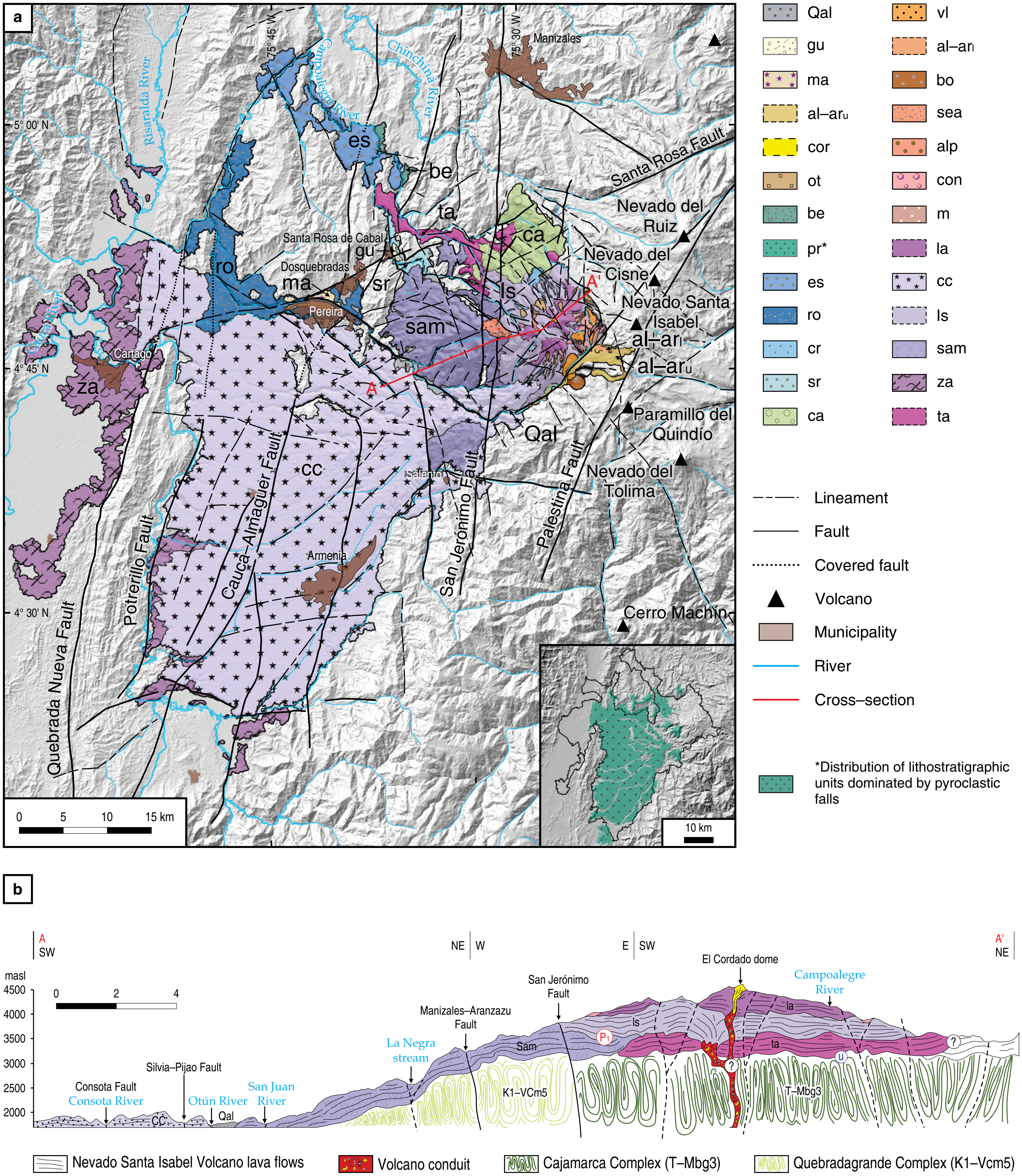

Figure 3. Schematic geological map and cross–section of the PSRVC merged on a shaded relief image of the study area (30 m resolution, NASA). **(a)** Distribution of the lithostratigraphic units recognized in the distal zone (labels of the stratigraphic succession can be found in Figure 4. The basement is represented by the areas with no colors). **(b)** SW–NE geological cross–section (A–A' in Figure 3a) that includes deposits of the Pre–PSRV and PSRV lithosomes.

1990; González & Núñez, 1991; McCourt et al., 1984; Mosquera et al., 1998; Nivia, 2001).

Isotopic dates presented in the literature (Neuwerth, 2009; Thouret, 1988; Thouret & van der Hammen, 1981; Thouret et al., 1997; Toro & Hermelín, 1991; van der Hammen, 1985) were used to support the PSRVC geochronology.

The main contribution of this chapter is a reconstruction of the eruptive history in addition to erosional, structural, and magmatic characteristics of the PSRVC and its interaction with other neighboring volcanoes. The geological history is established using systematic volcanic stratigraphy that is based on the application of traditional stratigraphic concepts adapted to the needs of the volcanological environment. Based on this approach, the geological map of the PSRVC provides valuable input for the evaluation of volcanic hazards. This study also seeks to evaluate the usefulness of the stratigraphic methodology in volcanic areas at low latitude (e.g., Pardo et al., 2019) and old volcanoes with high degrees of erosion and dense vegetation. If further information about the PSRVC is required, we encourage readers to refer to Pulgarín et al. (2017).

2. Geological Background

The PSRVC is located at 4° 47' 58.986" N and 75° 27' 28.081" W and is part of the North Volcanic Zone of South America (Gansser, 1973) and of the northern volcanic segment in the Colombian Central Cordillera in a region where the tectonic framework is associated with the geodynamics of the South American, Caribbean, and Nazca Plates together with the Coiba and Panamá microplates (Figure 1; Duque–Caro, 1990; Taboada et al., 2000). The PSRVC area lies between the Palestina, Cauca–Romeral, and NW–SE fault systems.

The PSRVC products discordantly overlap Mesozoic metamorphic rocks (Cajamarca and Arquía Complexes), Cretaceous volcanic and metasedimentary rocks (Quebradagrande Complex, Amaime Formation), Triassic igneous rocks (Pereira Gabbro Stock, Santa Rosa, Gabbro–Dioritic Stock), intrusive igneous rocks from the Upper Cretaceous (Navarco River Igneous Complex), and Oligocene – Miocene sedimentary rocks from a continental fluvial environment corresponding to the Cinta de Piedra (upper Oligocene), La Paila (lower Miocene), and La Pobreza (upper Miocene) Formations.

The Cajamarca Complex corresponds to rocks with low to medium degrees of metamorphism in the greenschist to amphibolite facies, which constitute part of the core of the Central Cordillera (e.g., Restrepo & Toussaint, 1985). The Arquía Complex is formed by garnet amphibolites, greenschists, and black schists, with Barrovian metamorphism (e.g., Restrepo & Toussaint, 1976). The Quebradagrande Complex is characterized by an elongated and discontinuous strip of Albian volcanic and metasedimentary rocks (e.g., Gómez–Cruz et al., 1995). The Pereira Gabbro Stock, Santa Rosa Gabbro–Dioritic Stock correspond to bodies of gabbros and diorites associated with the Romeral Fault System (e.g., González, 1993). The Amaime Formation is a sequence of basalts, pillow lavas, dikes, breccia, and tuffs from the Late Cretaceous (McCourt et al., 1984). The Navarco River Igneous Complex corresponds to intrusive igneous rocks (diorite and tonalite) from the Late Cretaceous (González & Núñez, 1991; McCourt et al., 1984). The Cinta de Piedra Formation is composed of a sequence of sandstones and claystones intercalated with horizons of conglomerates from the Late Oligocene (van der Hammen, 1960). La Paila Formation consists mainly of intercalations of conglomerates and dacitic tuffs from the Miocene (van der Hammen, 1960), and La Pobreza Formation corresponds to a sequence of conglomerates and sandstones from the Miocene (McCourt et al., 1984).

In this chapter, it is considered that the volcanic products of the Zarzal Formation are associated with the activity of the PSRVC. Regionally, this formation has been defined by Boussingault (1903), Nelson (1962), van der Hammen (1960), McCourt (1984), McCourt et al. (1984), Keith et al. (1988), Cardona & Ortiz (1994), Nivia (2001), and Suter (2008). The last author established that it corresponds to fine–grained (sands, silts, and clays) lacustrine sediments with the presence of diatomites, alternating with sands and gravels of fluvial domain and flows of volcanic products coming from the Central Cordillera.

The Quindío–Risaralda Fan (Guarín, 2008) is located to the west of the Central Cordillera in the Departments of Risaralda, Quindío, and northern Valle del Cauca (Figure 1). According to regional cartography (e.g., Caballero & Zapata, 1984; McCourt et al., 1985), the fan corresponds to volcaniclastic deposits that, initially, had a volcanic and glacial origins. Thouret (1988) suggested that the formation of this fan was related to volcanic and volcaniclastic events associated mainly with the activity of the PSRV and the Paramillo del Quindío Volcano (PQV).

3. Materials and Methods

This chapter is the result of time–consuming and detailed geological work that was conducted over 3 years, during which a total of 1154 sites were visited scattered across an area of 2150 km^2 within the Departments of Risaralda, Quindío, Caldas, and northern Valle del Cauca.

To describe and present the stratigraphy and the geological map, as well as the eruptive history of the PSRVC, we adapted the stratigraphic methodology proposed by Lucchi (2013), which establishes a stratigraphic framework for volcanic terrains that follows the common rules of the "International Stratigraphic Guide" (Salvador, 1994). Accordingly, lithostratigraphic units, lithosomes, and unconformities allowed to organize the stratigraphy framework, by the identification of the spatial and temporal relationships between volcanic products and prolonged quiescence intervals (volcano–tectonic collapses and intense episodes of glacial activity). These concepts allow correlation and greater understanding of the geological evolution of volcanoes.

Lithostratigraphic units are used in geological mapping to differentiate rock bodies forming discrete and recognizable units, based on the lithological properties and stratigraphic relations in a vertical succession (Salvador, 1994). Formations were defined in the PSRVC when all these principles were fulfilled. These units were described by means of lithofacies criteria based on distinctive lithologic characteristics (stratification, grain size, grain shape, sorting, fabric, and composition), description of the lateral or vertical variations in pyroclastic products induced by time, paleotopography, and increasing distance from the source. The nomenclature and classification of pyroclastic deposits and fragments following Fisher (1966), Schmid (1981), and Fisher & Schmincke (1984), whereas the nomenclature of Ingram (1954) was adopted for the strata thickness. Informal units were defined by identifying rock bodies with a distinctive 3D morphology by means of remote sensing because they were not accessible in the field due to dense vegetation and/or steep topography (cf. Pardo et al., 2019).

To characterize the components of lithostratigraphic units, 115 petrographic analyses were conducted using an Olympus BX51 microscope with a 5.0 Motic Cam and a PRIOR 123 model G point counter. Additionally, 107 geochemical analyses using x–ray fluorescence (XRF) techniques for major elements and the inductively coupled plasma mass spectrometry (ICP–MS) technique for trace elements were performed in the laboratories of the Servicio Geológico Colombiano.

Lithosomes were applied to identify and describe the main volcanic structures and eruptive sources during the evolution of the PSRVC based on the definition of Consiglio Nazionale delle Richerche Commissione per la Cartografia Geologica e Geomorfologica (1992), who described a lithosome as a rock body with defined morphology and associated with a specific genetic process. Therefore, defining lithosomes is valuable to identify the main volcanic edifices and nonvolcanic sources, as well as to illustrate the stratigraphic relationships of units from different eruptive sources (Lucchi, 2013). Lithosomes can frequently include two or more lithostratigraphic units composing a homogeneous 3D rock body or volcanic edifice, thus contributing to the definition of mappable units (although they are usually not directly represented on the map) (Lucchi, 2013). Notably, the study area is frequently characterized by the occurrence of depositional terraces found at various elevations along the main river channels around the PSRVC. These events commonly correspond to different episodes of accumulation of primary volcaniclastic deposits, lava products or epiclastic deposits. Different terraces are commonly associated with the corresponding lithostratigraphic units based on their distinctive lithology. In addition, some "external lithosomes" (Lucchi, 2013; Pardo et al., 2019) are introduced to identify volcanic bodies with geometry and thickness variations, clearly indicative of an adjacent and spatially connected or disconnected source area such as the PQV, the Alsacia–Arenero Volcanoes, and other sources of the San Diego–Cerro Machín Volcano–Tectonic Province.

The unconformities were defined based on erosive or non–depositional surfaces. These surfaces were differentiated on the basis of different hierarchical criteria for volcanic settings (Lucchi, 2013), particularly, considering the areal extent of the unconformity and the duration of the stratigraphic hiatus represented. A first–order unconformity (U) is recognized at a regional scale in the PSRVC and separates the PSRVC volcanic deposits from the metamorphic, plutonic, and sedimentary basement. Second–order (P_n) unconformities represent time gaps of volcanic inactivity, characterized by epiclastic sedimentation, erosion, flank collapses, and tectonic phases throughout the PSRVC region. Finally, the third–order unconformities (p_{ni}) are recognized only locally within the PSRVC and are associated with posteruptive intervals (related with destructive processes) or represent short intervals of quiescence among successive eruptions (Martí et al., 2018). The term "synthem" is not adopted here since it is preferable used to define larger unconformity–bounded units in the regional or interregional context (Chang, 1975; Salvador, 1994).

Lithostratigraphic units, lithosomes, and unconformities are then interpreted in terms of volcanic activity units, according to Fisher & Schmincke (1984), as continuous periods of activity separated by intervals of quiescence of different duration and size. The same authors pointed out that depending on the time range, the volcanic activity units can be differentiated into pulses (from seconds to minutes), phases (from minutes to days), eruptions (from days to years) or series of eruptions grouped into epochs (from tens to thousands of years) or periods (thousands to millions of years). Following Fisher & Schmincke (1984) and Lucchi (2013), these volcanic activity units are not adopted as mappable units because they are conceptual units that rely heavily on subjective interpretation.

To provide further chronostratigraphic information about the recognized lithostratigraphic and volcanic activity units, 31 isotopic ages were obtained, 22 by the ^{14}C method, and 9 by $^{40}Ar/^{39}Ar$, merged with other isotopic dating from the literature. These new ages allowed the eruptive history of the PSRVC to be rebuilt.

The $^{40}Ar/^{39}Ar$ data (Table 1) were conducted at the Oregon State University (in the USA) on plagioclase and the groundmass, for which rock samples with >2 wt % K content were used.

The necessary preparation and pretreatment of the sample materials for radiocarbon dating (Table 2) were carried out by the ^{14}C Laboratory of the Department of Geography at the University of Zürich. Datings were performed by AMS (accelerator mass spectrometry) with the accelerator in the Laboratory for Ion Beam Physics at the Swiss Federal Institute of Technology, Zürich. For paleosols, stable (old organic matter) and labile (young organic matter) fractions of the organic soil were analyzed (e.g., Eus-

Table 1. List of the $^{40}Ar/^{39}Ar$ isotopic ages obtained for volcanic products of the PSRVC.

Sample information				Results	Plateau		Normal isochron		Inverse isochron		Total fusion		
Sample code	Latitude N	Longitude W	Material	Age type	Age	± 2σ (i)	Age	± 2σ (i)	Age	± 2σ (i)	Age	± 2σ (i)	Lithostratigraphic units
							Intercept						
BPA–PSR–020	4° 46' 53.33"	75° 27' 36.10"	Plagioclase	Plateau Age	260.3	± 5.7 ka	270	± 13.6 ka	269.7	± 13.1 ka	274	± 3.3 ka	Las Águilas Formation
GRV–PSR–022	4° 46' 57.03"	75° 28' 25.38"	Plagioclase	Plateau Age	460.3	± 4.2 ka	468	± 5.2 ka	468.1	± 5.2 ka	454	± 4.7 ka	La Sierra Formation
MTA–PSR–049	4° 46' 12.46"	75° 29' 28.07"	Plagioclase	Plateau Age	470.3	± 6.5 ka	480	± 19.1 ka	479.6	± 18.5 ka	468	± 5.0 ka	La Sierra Formation
GVR–PSR–068	4° 44' 21.67"	75° 27' 22.78"	Plagioclase	Plateau Age	498.4	± 5.0 ka	486	± 19.9 ka	484.8	± 19.5 ka	498	± 4.6 ka	La Sierra Formation
GVR–PSR–068	4° 44' 21.67"	75° 27' 22.78"	Ground-mass	Plateau Age							518	± 1.7 ka	La Sierra Formation
GVR–PSR–106	4° 52' 7.78"	75° 29' 45.74"	Plagioclase	Plateau Age	502.9	± 4.8 ka	499	± 13.3 ka	500	± 12.8 ka	502	± 3.6 ka	La Sierra Formation
ACT–PSR–015	4° 47' 12.03"	75° 26' 5.59"	Plagioclase	Plateau Age	535.9	± 7.7 ka	538	± 20.0 ka	546.5	± 18.1 ka	524	± 7.0 ka	La Sierra Formation
GVR–PSR–005	4° 48' 12.50"	75° 27' 43.49"	Plagioclase	Plateau Age	568.1	± 12.7 ka	569	± 29.4 ka	573.2	± 28.6 ka	532	± 9.1 ka	La Sierra Formation
GVR–PSR–005	4° 48' 12.50"	75° 27' 43.49"	Ground-mass	Plateau Age							550	± 3.1 ka	La Sierra Formation

The $^{40}Ar/^{39}Ar$ dating was conducted at Oregon State University (USA) on plagioclase and the groundmass, and rock samples with >2 wt % K content were used.

terhues et al., 2003; Favilli et al., 2009a, 2009b; Helfrich et al., 2007; Kögel–Knabner et al., 2008) to ensure greater accuracy of the data. Due to the high variability of organic structures and the behavior of soils, ages may have differed completely from years to millennia. When the ^{14}C dating was related to the bulk soil, only an 'average' age of soil organic matter was obtained.

For the geomorphological analysis, 31 flight lines of aerial photographs with scales from 1:20 600 to 1:60 000 were interpreted. Likewise, UAVSAR (uninhabited aerial vehicle synthetic aperture radar) images, courtesy NASA/JPL–Caltech (National Aeronautics and Space Administration/Jet Propulsion Laboratory–California Institute of Technology; https://asterweb.jpl.nasa.gov/gdem.asp) from a 30 m–resolution DEM (digital elevation model) and a 12.5 m resolution DEM were used (JAXA, 2012). Additionally, the topographic base of the Instituto Geográfico Agustín Codazzi was used, with scales of 1:25 000 and 1:100 000. Finally, data from this interpretation were correlated with geological field data. The information was analyzed and processed using the ArcGIS v. 10.2 software (v. 10.2.2 and 10.2.3; ©Esri, 2014).

4. Results

4.1. Morphological Setting

We define two major overlapping composite volcanic edifices named Pre–Paramillo de Santa Rosa (Pre–PSRV) with calculated ages from ca. 2.3–0.57 Ma and PSRV that presumably started its development at ca. 0.57 Ma and extended into the Holocene, including a coulée–lava dome emplaced during the Holocene. These edifices have undergone processes of weathering, erosion, reworking, and have been affected by glacial, glaciofluvial, fluvial, and tectonic dynamics that have constantly shaped the landscape of the PSRVC. The NW and W flanks of the PSRV edifice exhibit local collapses, which are linked to debris avalanche deposits. A very extensive and eroded fan geoform is associated with the W–SW side of this complex, distributed to the distal zone. The glacial paleorelief stands out from 3600 masl, forming elongated glacial valleys and extensive moraine deposits. The PSRVC is the westernmost structure of the San Diego–Cerro Machín Volcano–Tectonic Province

Table 2. List of the ^{14}C ages obtained by accelerator mass spectrometry at the University of Zürich (Switzerland) for paleosols, charcoal, peat, and wood fragments related to products.

Sample code	Latitude N	Longitude W	Elevation (masl)	Sample type	^{14}C year BP	±1σ	Calibrated age (cal year BP) 1 sigma –68.2%	2 sigma –95.4%	Lithostratigraphic units
JCH–PSR–065–E–3–2	4° 49' 09.11"	75° 43' 46.35"	1335	Soil**	1782	25	1732–1626	1813–1618	External pyroclastic falls (Holocene)
JCH–PSR–063–A–3	4° 49' 18.10"	75° 45' 17.46"	1324	Soil*	2368	24	2423–2345	2463–2341	External pyroclastic falls (Holocene)
JCH–PSR–065–E–3–1	4° 49' 09.11"	75° 43' 46.35"	1335	Soil*	2585	27	2750–2728	2763–2547	External pyroclastic falls (Holocene)
ACT–PSR–021–G–3	4° 45' 36.84"	75° 26' 36.90"	3903	Soil*	3109	23	3368–3260	3382–3249	External pyroclastic falls (Holocene)
BPA–PSR–009–G–3	4° 45' 53.51"	75° 25' 59.08"	3962	Peat	4666	36	5463–5320	5571–5314	El Mosquito Formation
BPA–PSR–009–I–3	4° 45' 53.51"	75° 25' 59.08"	3962	Peat	4962	36	5730–5648	5853–5602	El Mosquito Formation
VNRLM–104–A–3	4° 36' 48.03"	75° 38' 48.80"	1754	Soil*	5198	30	5988–5920	5995–5910	External pyroclastic falls (Holocene)
MTA–PSR–064–E–3	4° 47' 23.22"	75° 24' 37.08"	3942	Charcoal	6583	37	7506–7436	7564–7428	Otún Formation
JCH–PSR–063–C–2–3	4° 49' 18.10"	75° 45' 17.46"	1324	Soil**	6597	29	7556–7544	7564–7433	External pyroclastic falls (Holocene)
ACT–PSR–021–K–3	4° 45' 36.84"	75° 26' 36.90"	3903	Soil*	7152	29	7998–7954	8016–7936	Valle Largo Formation
GVR–PSR–064–D–3	4° 45' 27.85"	75° 27' 47.52"	4111	Soil*	7192	38	8022–7965	8154–7940	Valle Largo Formation
JCH–PSR–063–C–1–3	4° 49' 18.10"	75° 45' 17.46"	1324	Soil*	8395	28	9473–9420	9490–9311	External pyroclastic falls (Holocene)
GVR–PSR–113–K–3	4° 51' 46.26"	75° 29' 48.42"	3095	Soil*	22 812	84	27 315–27 085	27 430–26 938	Potreros–Porvenir–El Roble Formation
GVR–PSR–116–R–3	4° 51' 24.41"	75° 29' 59.72"	3134	Soil**	30 489	223	34 670–34 240	34 866–34 037	Potreros–Porvenir–El Roble Formation
VNRLM–103–B2–3	4° 42' 23.70"	75° 36' 23.99"	2010	Soil*	31 723	222	35 903–35 347	36 138–35 090	Potreros–Porvenir–El Roble Formation
YCT–PSR–126–3	4° 59' 28.59"	75° 38' 30.66"	1209	Charcoal	31 937	218	36 195–35 608	36 310–35 329	Betania Formation
VNRLM–103–C	4° 42' 23.70"	75° 36' 23.99"	2010	Charcoal	40 881	615	44 990–43 842	45 530–43 311	Potreros–Porvenir–El Roble Formation
VNRLM–103–A1–3	4° 42' 23.70"	75° 36' 23.99"	2010	Wood	44 245	299	47 911–47 014	48 383–46 619	Potreros–Porvenir–El Roble Formation
VNRLM–103–A2–3	4° 42' 23.70"	75° 36' 23.99"	2010	Soil**	>45 000		>49 000	>49 000	Potreros–Porvenir–El Roble Formation
YCT–PSR–027–B–3	4° 52' 47.30"	75° 27' 54.80"	3014	Soil**	45 709	1326	50 229–48 172	51 826–47 171	Potreros–Porvenir–El Roble Formation

Table 2. List of the ^{14}C ages obtained by accelerator mass spectrometry at the University of Zürich (Switzerland) for paleosols, charcoal, peat, and wood fragments related to products (*continued*).

Sample code	Latitude N	Longitude W	Elevation (masl)	Sample type	^{14}C year BP	±1σ	Calibrated age (cal year BP) 1 sigma –68.2%	2 sigma –95.4%	Lithostratigraphic units
VNRLM–103–B2–3	4° 42' 23.70"	75° 36' 23.99"	2010	Soil**	>46 000 (48 537)	1587	>49 000		Potreros–Porvenir–El Roble Formation
MTA–PSR–109–D–3	4° 51' 35.56"	75° 28' 50.61"	3141	Charcoal	48 398	1772	50 530–46 715	53 439–45 325	Potreros–Porvenir–El Roble Formation

Calibration ages by the laboratory: OxCal v4. 2.4 Bronk Ramsey (2013); r:5; IntCal13 atmospheric curve (Reimer et al., 2013).

*Stable fraction of organic soil (H_2O_2). **Labile fraction of organic soil (POM).

The ages in gray are over the limit of the method.

The necessary preparation and pretreatment of sample materials for radiocarbon dating were carried out by the ^{14}C Laboratory of the Department of Geography at the University of Zurich (GIUZ). The dating itself was done by AMS (accelerator mass spectrometry) with the accelerator in the Laboratory for Ion Beam Physics (LIP) at the Swiss Federal Institute of Technology, Zurich (ETH).

and lengthens in a SW–NE direction, parallel to the main Palestina Fault System.

4.2. Volcanic Unconformities

Erosional and non–depositional discordances with variable duration times and areal distributions are recognizable in the stratigraphy of the PSRVC, representing significant hiatuses or gaps in the stratigraphic succession. The first–order unconformity (U) has a regional extent and is represented by the nonconformity between the volcanic products of the PSRVC (and interlayered volcaniclastic and epiclastic deposits) and the crystalline basement. In the proximal area of the PSRVC, U marks the contact with Mesozoic metamorphic rocks of the Cajamarca Complex and Cretaceous volcanic and metasedimentary rocks of the Quebradagrande Complex. This unconformity can potentially be traced along the entire Central Cordillera of Colombia and to the south into Ecuador at the contact between the products of different volcanic edifices and the metamorphic basement (cf. Pardo et al., 2019). In the distal area, the first unconformity is represented by the nonconformity between the Quindío–Risaralda Fan and Mesozoic metamorphic rocks of the Arquía Complex, Triassic igneous rocks of the Pereira Gabbro Stock, Santa Rosa Gabbro–Dioritic Stock, Upper Cretaceous volcanic rocks of the Amaime Formation, intrusive igneous rocks from the Upper Cretaceous of the Navarco River Igneous Complex. Also, it is represented by a disconformity with Oligocene – Miocene continental fluvial sedimentary rocks corresponding to the Cinta de Piedra, La Paila, and La Pobreza Formations. The second–order unconformities P_{1-3} are erosive disconformities formed during the prolonged intervals of quiescence of the PSRVC throughout the study area, at times including glacial erosion and the associated deposits. Two third–order unconformities (p_{1a-b}), associated with minor quiescence intervals and gravitational collapses of the S–SW and W flanks of volcanic edifice PSRV, are recognized in localized portions of the study area. These are angular unconformities in the areas of the collapses and commonly change with distance to low–angle unconformities and disconformities. In the study area, these unconformities are best traced in proximal areas.

The history of the PSRVC includes 26 lithostratigraphic units that constitute two major overlapping volcanic edifices: The Pre–PSRV and the PSRV, and some external lithosomes related to different eruptive sources located outside the study area. The main features of the PSRVC stratigraphic succession are hereafter described according to the main lithosomes, lithostratigraphic units, and unconformities defined. An interpretation of the lithostratigraphic units in terms of the main eruptive processes and transport/depositional mechanisms is also provided for the volcanic rocks.

On the map, effusive products are represented by solid color polygons, and volcaniclastic products are represented with hatched pattern.

In Figure 4, lithostratigraphic units are represented according to their reconstructed stratigraphy and isotopic ages. We

Figure 4. Schematic stratigraphic succession of the PSRVC showing the main unconformities (with a synthetic explanation of their nature), lithosomes, and lithostratigraphic units. The ages of the mapped units are shown in a proper column. The interpreted succession of eruptive periods and epochs, posteruption and inter–eruption times, as well as their constructive to destructive characters, are also indicated.

Unconformity category	Lithosome	Acronym	Litostratigraphic unit	Age	Product/deposit	Strathigraphic range	Main steps of evolutive history	Period
		Qal	Undifferentiated recent deposits		Alluvial deposits		Post–eruptive processes	Period 2
		gu	Guacas Formation		Epiclastic deposits			
		ma	Matecaña Formation	1782 ± 25 y BP (1) 2585 ± 27 y BP (1)				
		mo	El Mosquito Formation	4666 ± 36 y BP (1) 4962 ± 36 y BP (1)	Fluvial–lacustrine deposits			
	Al–Ar	al–ar$_u$	Upper Alsacia–Arenero Formation		External lava flows		Eruptive epoch 2.4	
	PSRV	cor	El Cordado geomorphological unit		Coulée–dome			
		ot	Otún Formation	6121 ± 37 y BP (1) 6583 ± 37 y BP (1)	PDCs deposits			
		vl	Valle Largo Formation	7152 ± 29 y BP (1) 7192 ± 36 y BP (1)	PDCs and pyroclastic falls deposits			
	Al–Ar	al–ar$_l$	Lower Alsacia–Arenero Formation		External lava flows			
	PQV	bo	El Bosque Formation		Debris avalanche deposits		Post–eruptive time	
		sea	San Eugenio Alto unit					
		alp	Los Alpes Formation					
P3	PSRV		Glacial erosion unconformity associated to the early and late Otún stage					
		con / m	El Cóndor Formation	10.5–11.5 ka (7) 12.5–13.5 ka (7)	Glacial and glaciofluvial deposits (m: moraine)		Early and late Otún glacial stages	
		be	Betania Formation	31 937 ± 218 y BP (1)	PDCs deposits		Eruptive epoch 2.3	
	SCVTP	pr	Potreros–Porvenir–El Roble Formation	22 812 ± 84 y BP (1) 31 723 ± 222 y BP (1) 45 709 ± 1326 y BP (1)	External pyroclastics			
P2	Paramillo de Santa Rosa Volcano (PSRV)		Glacial erosion unconformity associated to the maximum glacial extent of the last glaciation					
		es	La Esmeralda Formation	45–25 ka (6) 48–28 ka (5)	Lahar deposits		Glacial erosion and reworking during the maximum glaciation extent of the last glaciation	
		ro	La Romelia–El Pollo Formation					
		cr	La Cristalina unit		Glacial and glaciofluvial deposits			
P1b			Volcano–tectonic unconformity associated to W flank collapses of PSRV					
		sr	Santa Rosa Formation	>40 000 y BP (4)	Lahar deposits		Post–eruptive time	
		ca	Campoalegre Formation	>48 398 ±1772 y BP(1)	Debris avalanche deposits			
		la	Las Águilas Formation	260.3 ± 5.7 ka (1)	Lava flows		Eruptive epoch 2.2	
P1a			Volcano–tectonic unconformity associated to S–SW flank collapses of PSRV					
		cc	Cedral–Ceilán Formation		Debris avalanche, lahar, and epiclastic deposits.		Post–eruptive time	
		ls	La Sierra Formation	460.3 ± 4.2 ka (1) 470.3 ± 6.5 ka (1) 502.9 ± 4.8 ka (1) 535.9 ± 7.7 ka (1) 568.1 ± 12.7 ka (1)	Lava flows		Eruptive epoch 2.1	
P1			Erosional unconformity associated to prolonged stratigraphic hiatus					
	Pre–Paramillo de Santa Rosa Volcano (Pre–PSRV)	sam	Samaria Formation		PDCs and lahar deposits		Eruptive epoch 1.2 Successive eruptions separated by times of repose	Period 1
		za	Zarzal Formation (Volcaniclastic facies)	0.79 ± 0.22 Ma (3) 1.06 ± 0.17 Ma (3) 1.32 ± 0.07 Ma (3) 2.05 ± 0.60 Ma (3)	Volcaniclastic deposits interspersed with layers of sadstones, siltstones, claystones, and volcanic polymitic conglomerates.			
		ta	Tarapacá Formation	2.3 ± 0.1 Ma (2)	Lava flows		Eruptive epoch 1.1	
U			Regional non–conformity between the volcanic products of PSRVC (and interlayered volcaniclastic and epiclastic deposits) and the non–volcanic basement.					

Basement formed by Mesozoic metamorphic rocks (Cajamarca and Arquía complexes), Cretaceous metavolcanic rocks, and metasedimentary (Quebradagrande Complex), Triassic igneous rocks (Pereira Gabbro Stock, Santa Rosa Gabbro–Dioritic Stock), and Oligocene – Miocene sedimentary rocks of fluvial continental enviroment from Cinta de Piedra, La Paila, and La Pobreza Formations.

(1) Ages obtained in this work; (2) Thouret (1988); (3) Neuwerth (2009); (4) Toro & Hermelín (1991); (5) Thouret et al. (1997); (6) van der Hammen (1985); (7) Thouret & van der Hammen (1981).

include information on eruptive sources, correlations, lateral variations of facies, age ranges or uncertainty (showed as double–head arrows for the cases of unprecised stratigraphic relationships or geochronology) and interpretations in terms of volcanic activity units.

4.3. Stratigraphic Succession

4.3.1. Pre–Paramillo de Santa Rosa Volcano Lithosome

The Pre–PSRV lithosome consists of lava flow emplacements, concentrated pyroclastic density currents (PDCs), and lahars, all grouped in the Tarapacá Formation and the Samaria Formation. These deposits discontinuously crop out in the W, NW, and SW sectors of the study area. The Tarapacá Formation consists of a succession of andesitic (60.23 to 61.87 wt % SiO_2) and dacitic (63.48 to 64.93 wt % SiO_2) lava flows, which exhibit massive, blocky, and surficial breccia structures, sometimes with subhorizontal cooling planes. Lava flows have medium to fine–grained porphyritic textures, in which the plagioclase microphenocrysts appear against the dominant cryptocrystalline groundmass. These rocks present an association of plagioclase, clinopyroxene, orthopyroxene, and amphibole as accessory mineral, with abundant pseudomorphs of opaque minerals replacing amphiboles. This lava flow succession extends to the NW and W up to 20 km, covering an area of approximately 30 km^2, reaching a maximum thickness of 200 m, and forming flattish plateaus (in inverted relief) along the flanks of the PSRVC. These lavas are dated by K/Ar (whole–rock) at 2.3 ± 0.1 Ma by Thouret (1988) in the Potreros locality (W of the PSRVC; Figure 5a). The Samaria Formation is composed of deposits of concentrated PDCs and lahars that are strongly dissected and clearly affected by weathering, erosion, and redeposition processes in the W and SW sectors of the PSRVC, resulting in a succession of variable thickness (5–100 m). Deposits of concentrated PDCs are massive, strongly weathered, poorly sorted, and matrix–supported, with angular to subrounded andesite blocks with fine to medium–grained porphyritic textures. They also contain pumice and lapilli embedded in a vitro crystalline matrix. These deposits are highly weathered and altered (Figure 5d, 5e), exhibiting manganese oxide concentrations (Figure 5c). These PDCs are characterized by a transition from proximal to distal areas. Locally, these deposits are covered by lahar deposits that are massive to poorly stratified, matrix–supported, poorly sorted, and composed of volcanic fragments of a variety of grain sizes (gravels to thick blocks), subrounded to rounded in shape. The thicknesses vary from 5 to 50 m along the San Juan (Figure 5b) and San Eugenio Rivers, Callejones and Volcanoes streams, and La Florida and Pez Fresco localities (Pereira). In distal areas such as Cartago, La Virginia, Montenegro, and SE of La Tebaida, approximately 50 km from the PSRV summit area, the lahar deposits of the Samaria Formation are represented by medium to thick (0.8 to 5 m) massive and matrix–supported beds, which are interlayered with very thin to medium sandstone beds, finely laminated siltstones, claystones, and volcanic polymictic conglomerates dated by Neuwerth (2009) at 2.05 ± 0.60 Ma, Ma, 1.32 ± 0.07 Ma, and 0.79 ± 0.22 Ma ($^{40}Ar/^{39}Ar$, crystallization ages in biotite). These lahar deposits have moderate sorting, with altered pumice and porphyritic lithic fragments that are predominantly subrounded to rounded and contain boulders and gravel sizes within a silty–sandy matrix.

The surfaces of subaerial erosion on the Tarapacá and Samaria Formations are associated with the prolonged time of inactivity recorded by the second–order unconformity P_1.

4.3.2. Paramillo de Santa Rosa Volcano Lithosome

The PSRV lithosome includes the current edifice of the PSRVC; other minor lithosome is associated with a dome extrusion to the north of the PSRV during its evolution (Figure 2a–c). A few volcanic exogenous lithosomes are defined to identify volcanic bodies of external provenance, which are characterized by a distinctive 3D geometry associated with the activity of the PQV, the Alsacia–Arenero Volcanoes, and other volcanic sources of the San Diego–Cerro Machín Volcano–Tectonic Province (the last one considered as a single exogenous lithosome, until the volcanic source of each deposit is later determined).

La Sierra Formation is composed of a succession of andesitic (59.33 to 62.91 wt % SiO_2) and dacitic (63.08 to 65.67 wt % SiO_2) lava emplacements, with the former predominant; these units commonly contain basal autobreccias, cooling structures, and banding. The lava flows show porphyritic texture and a mineral assemblage of plagioclase, clinopyroxene, and orthopyroxene, with opaques, apatite, and amphibole as accessory minerals, and chlorite as an alteration mineral. The lava succession reaches a maximum thickness of 200 m. This unit is

→

Figure 5. Geological evidence of the early volcanic products in the study area. **(a)** Lava flows of the Tarapacá Formation, with staggered lobe–like morphology, reaching up to 270 m in height along the Campoalegre River basin in the Potreros locality, lying on the regional unconformity (U) over Cretaceous rocks of the Quebradagrande Complex. The red arrow shows the approximate location of the K/Ar (whole–rock) date of 2.3 ± 0.1 Ma from Thouret (1988). **(b)** Lahar deposits of the Samaria Formation. Facies are clast–supported near the base and matrix–supported towards the top. **(c)** Volcaniclastic deposits of the Samaria Formation characterized by a higher concentration of manganese oxides (MnO_2) in the SW sector of the PSRVC. **(d)** Strongly weathered and varicolored deposits of the Samaria Formation in the Cedral area. **(e)** Detail of the volcaniclastic deposits of the Samaria Formation with angular fragments and vesicular clasts in the La Variante (Otún River) locality. Scales in cm.

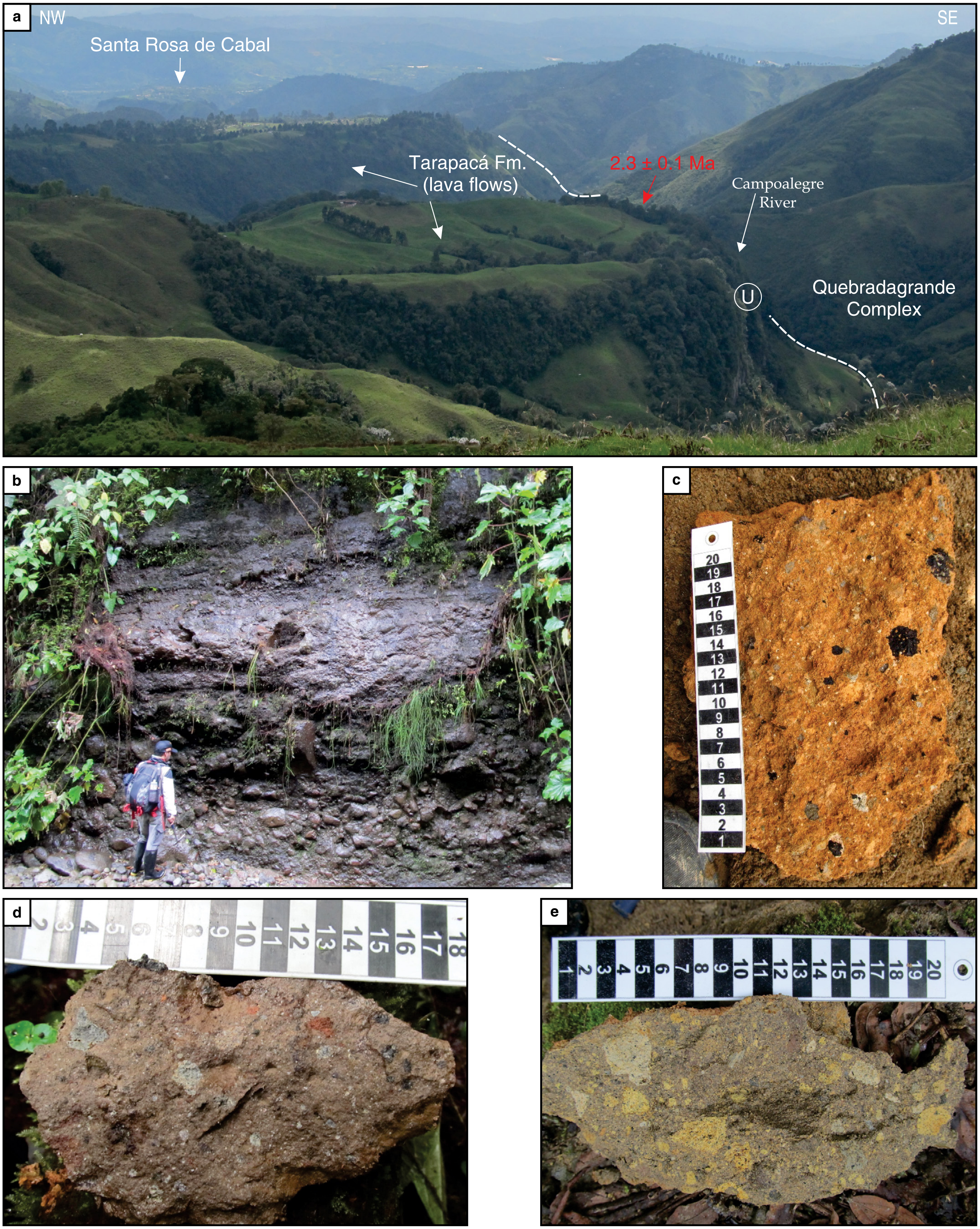
a
NW
SE
Santa Rosa de Cabal
Tarapacá Fm.
(lava flows)
2.3 ± 0.1 Ma
Campoalegre
River
U
Quebradagrande
Complex
b
c
d
e

affected by a series of NW–SE tectonic structures parallel to La Cristalina and Los Pájaros streams, and the Campo Alegrito and San Ramón Rivers. $^{40}Ar/^{39}Ar$ dates for these lava emplacements are obtained at 568.1 ± 12.7 ka, 535.9 ± 7.7 ka, 502.9 ± 4.8 ka, 498.4 ± 5.0 ka, and 470.3 ± 6.5 ka.

Stratigraphically above La Sierra Formation lavas, the Cedral–Ceilán Formation consists of widespread deposits of debris avalanche, and lahars and local epiclastic deposits. These deposits crop out towards the SSW of the PSRVC, between the Barbo and Otún Rivers and along the Quindío–Risaralda Fan, filling a paleovalley formed by relicts of the older Samaria Formation.

The debris avalanche deposits (Figure 6) form the base of the unit with variable thicknesses (from several to 200 m) along the basins of the Otún, Barbo, Consota, Barbas, El Roble, and Quindío Rivers, the Cestillal, Boquía, and Buenavista streams, and as far as the vicinity of their discharges into the Cauca and La Vieja Rivers. Deposits are dark to light gray in color, hardened and massive, monolithological to locally heterolithological, with moderate sorting gradually passing from clast–supported to matrix–supported facies (Figure 6b). Clasts (from centimeters to meters) are mainly lavas (andesites) and minor plutonic and metamorphic lithic fragments, angular to subangular (Figure 6c) and embedded in a hardened lithic matrix. They typically show macroscopic (Figure 6a, 6d) and microscopic jigsaw structures, radial cracks, and shattered blocks. Additionally, it is common to find them saprolitized (Figure 6e), with thicknesses of up to 30 m along the main river channels of the Consota and El Roble Rivers and the Boquía and Buenavista streams.

Considering their areal distribution towards the SSW, these debris avalanche deposits are presumably related to successive gravitational collapses of the S–SW and W flanks of the PSRV. The deposits of lahars, locally, overlie the deposits of avalanches forming the upper portion of the Cedral–Ceilán Formation. Lahars have an average thickness of 50 m, and they are massive (Figure 7a) or graded (normal or reverse) and contain predominantly volcanic rocks (lavas) with some metamorphic clasts from the basement. In distal areas, the lahar deposits show parallel flat stratification and imbrication (Figure 7b). In some places, debris avalanche and lahar deposits of the Cedral–Ceilán Formation are overlaid disconformably (Figure 7c) by strongly weathered and oxidized (Fe_2O_3 and MnO_2) epiclastic deposits (Figure 7d), occasionally including lenses and intraclasts of paleosols and volcanic ash.

The gravitational collapses of the S–SW and W flanks of the PSRV defined in this unit are associated with deposits of debris avalanches, lahars and epiclastic deposits, and the volcanic inactivity is interpreted as a third–order unconformity, p_{1a}.

Bounded at the base by the third–order unconformity, p_{1a}, Las Águilas Formation is made up of a thick (up to 100 m) succession of andesitic (59.77 to 62.71 wt % SiO_2) and dacitic (63.08 to 64.70 wt % SiO_2) lava flow units cropping out in the more proximal area of PSRV (Figure 8). These lava emplacements are characterized by ogives as surface structures, but within their bodies, they may also exhibit basal breccias, horizontal cooling joints, and massive structures. The prevailing textures of these rocks are porphyritic and hypocrystalline; the rocks show low to moderate degrees of alteration, and the main mineral assemblage includes plagioclase, orthopyroxene, and clinopyroxene; amphibole, apatite, and opaque as accessory minerals, and sparse chlorite as an alteration mineral. The $^{40}Ar/^{39}Ar$ dating of plagioclase yields an age of 260.3 ± 5.7 ka.

Stratigraphically above Las Águilas Formation, debris avalanche deposits of the Campoalegre Formation are distributed to the W and NW of the PSRV, along segments of the Campoalegre and Campo Alegrito Rivers basins, as well as La Cristalina stream; they cover an area of 54 km^2 and are related to a W–dipping flank collapse of the PSRV. These deposits typically exhibit numerous hummocks in El Porvenir and La Tigrera localities, together with megaclasts (up to 10 m) and toreva blocks (up to 200 m in diameter). The deposits are characterized by a high degree of weathering, with andesitic volcanic block–sized fragments with jigsaw structures. An age >48 398 ± 1772 years BP is suggested for this unit based on AMS ^{14}C dating from PDCs that overlie it in El Porvenir locality.

Stratigraphically, the debris avalanche deposits of the Campoalegre Formation are presumably coeval with the lahar deposits of the Santa Rosa Formation, cropping out in the municipality of Santa Rosa de Cabal, along the San Eugenio River and La Leona stream. Two amalgamated lahar layers are recognized. One of them is mainly massive and slightly hardened, it shows a blue–green coloration with metamorphic and volcanic fragments and wood remnants that have an age >40 000 years BP, according to Toro & Hermelín (1991). The other lahar layer is tan colored, more altered than the lower layer and includes volcanic (both dense clasts with porphyritic texture and rounded pumice) and metamorphic fragments.

The Campoalegre Formation debris avalanche deposits (and subsequent lahars) and the corresponding W–dipping flank collapse of PSRV are considered representative of the third–order unconformity, p_{1b}.

Glacial and glacial–fluvial deposits associated with La Cristalina unit crop out to the W of the PSRVC at the headwaters of the Campo Alegrito River and La Cristalina and Los Pájaros streams, as well as to the SE along the Agua Blanca stream and in the Barbo River basin. Some of these deposits correspond to moraines (Figure 8), the lower fronts of which are visible at elevations between 3000 and 3300 masl In the municipalities of Pereira, Dosquebradas, and Chinchiná in the Otún, San Eugenio, and Campoalegre Rivers basins, debris flow deposits of La Romelia–El Pollo and La Esmeralda Formations correspond to depositional terraces with moderately dissected flat tops crests. These deposits are mainly composed of volcanic and basement (less abundant) fragments (green and black schists, gabbros, and basalts).

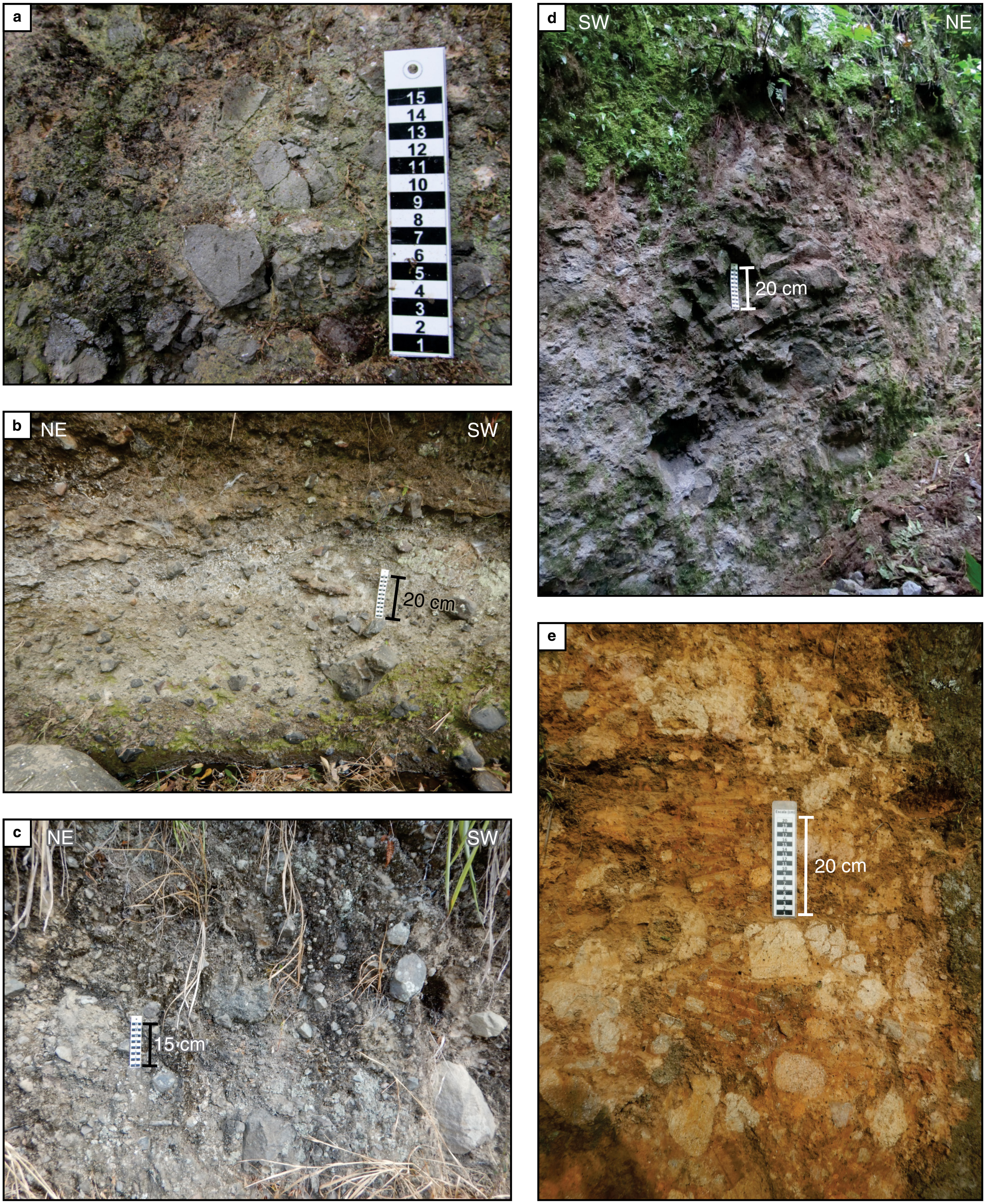

Figure 6. Debris avalanches and lahars, together with epiclastic deposits of the Cedral–Ceilán Formation. **(a)** cm–sized jigsaw fragments. **(b)** Matrix–supported facies in the Navarco locality. **(c)** Palmares locality sector (La Tebaida). Despite the distance, the predominance of angular fragments continues. **(d)** Blocks with jigsaw structures in La Variante locality. **(e)** Saprolite of the debris avalanche deposit in Quimbaya at the Buenavista River bridge. Scale in cm.

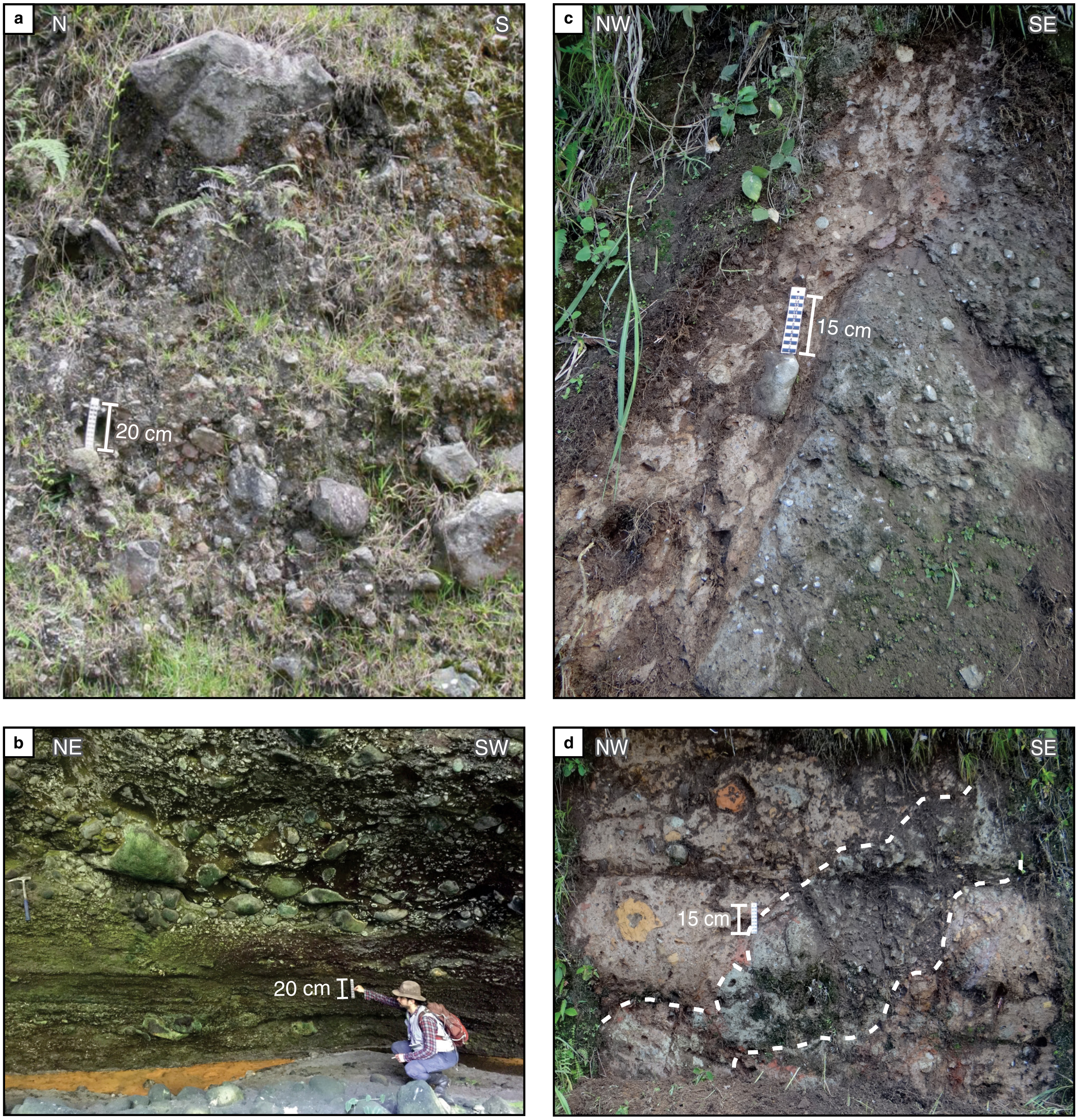

Figure 7. Lahars and epiclastic deposits of the Cedral–Ceilán Formation. **(a)** Massive facies deposits of debris flow in the upper part of the Barbas River (El Manzano sector). **(b)** Lahar deposits with parallel flat stratification overlaid by matrix– to clast–supported deposits. Outlet of Piedras stream to La Vieja River. **(c)** La Arabia sector epiclastic deposits, left bank of the Barbo River. Note the strong alteration of the deposits (top left) and the net contact with the debris avalanche deposits. **(d)** Epiclastic deposits involving large fragments of debris avalanche deposits (dotted line) in La Arabia locality.

The unconformity P_2 is the glacial erosion surface carved on the PSRV edifice during the maximum glacial extent (and associated deposits) in Colombia.

The exogenous lithosome of the San Diego–Cerro Machín Volcano–Tectonic Province generated pyroclastic fallout deposits, which are currently embedded on the actual surface of the PSRVC. These deposits (Potreros–Porvenir–El Roble Formation) are composed of thin to medium layers with a tabular geometry reaching a total thickness of up to 20 m and pyroclastic deposits that are light tan to brown in color with fine lapilli

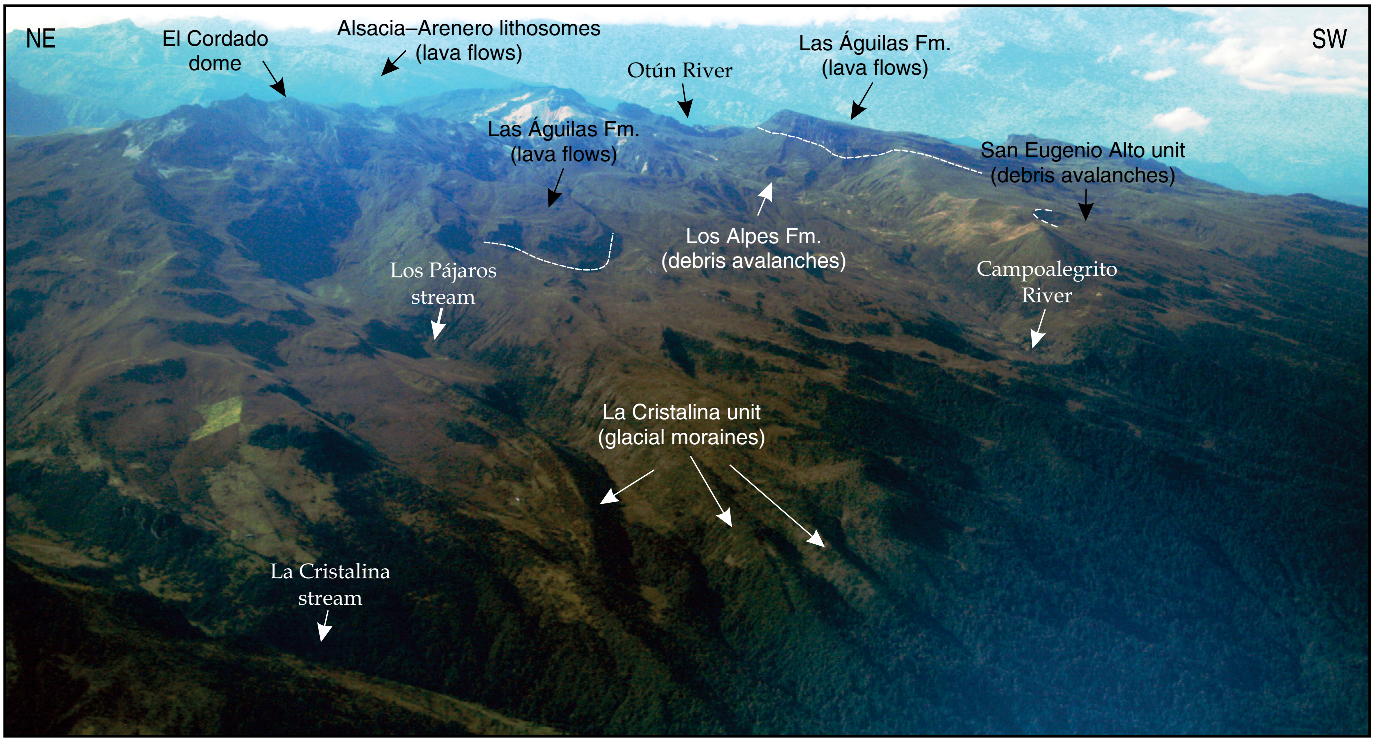

Figure 8. Geomorphological features and lithostratigraphic units along the W flank of the Paramillo de Santa Rosa Volcanic Complex in an overflight photograph. (Fm.) Formation.

to very fine ash that contains glass, plagioclase crystals, some ferromagnesian minerals and, rarely, biotite. These deposits are distributed to the W and SW of the PSRVC (Figure 3a), becoming part of the oldest lapilli–ash layers on the upper portion of the Quindío–Risaralda Fan (Figure 9a) and are characterized by a high level of alteration. Ages within the Late Pleistocene are suggested (Table 2).

Stratigraphically above, concentrated PDC deposits of the Betania Formation are found, cropping out in the Campo Alegrito River basin in the Betania sector (in the proximal area), which lie on lava flows of La Sierra Formation. These deposits are massive, matrix–supported, poorly sorted, moderately welded, and characterized by varying degrees of weathering. They are composed of lapilli–size pumice (some with *fiamme* structures), accessory volcanic lithic fragments (porphyritic lava) that are angular to subangular and embedded within a vitric–crystal–lithic matrix. In La Ínsula sector (distal area), on the right bank of the Campoalegre River, the Betania Formation gradually passes into lahar deposits characterized by pumice lapilli and rounded dense lithic blocks mainly of volcanic rocks (fine porphyritic lava) and sparse plutonic and metamorphic rocks, embedded within a lithic–crystalline ash matrix, with charcoal fragments (reworked) dated at 31 937 ± 218 years BP by ^{14}C.

At elevations higher than 3100 masl, near to the headwaters of the Campoalegre River (to the W) and in the basins of the Sinú and El Cóndor streams (to the E), moraines and glacial–fluvial deposits from El Cóndor Formation (Figure 10a) are mapped. The moraines (lateral and terminal) are up to 2.4 km long and approximately 100 m thick, are massive, matrix–supported, and poorly sorted and contain rounded porphyritic lava blocks up to 3 m in diameter. Glacial–fluvial deposits filled the wide glacial valleys, showing overall normal grading. According to the elevations of the moraine fronts (Thouret & van der Hammen, 1981), these deposits are associated with the early and late Otún glacial stages and mark a prolonged interval of volcanic inactivity recorded as the second–order unconformity P_3.

Above the second–order unconformity P_3, there are the youngest volcanic products of PSRV and external lithosomes, together with debris avalanche, lahar, and epiclastic deposits. All these deposits have not been affected by substantial glacial erosion and sculpting.

The debris avalanche deposits of Los Alpes Formation and San Eugenio Alto unit crop out in the W and SW sectors of the PSRV (Figure 8). These deposits reach up to 3 km long and cover areas of 0.8 and 4.5 km^2, respectively. Los Alpes Formation deposit comprises megablocks and blocks of porphyritic andesitic lavas, with some jigsaw blocks embedded in a hydrothermally altered, clayish–sandy matrix.

Los Alpes Formation and San Eugenio Alto unit could, therefore, be stratigraphically coeval with the debris avalanche deposits of El Bosque Formation that was generated by the massive landslide in the W flank of the PQV, the deposits of which crop out in a morphologic depression and are characterized by

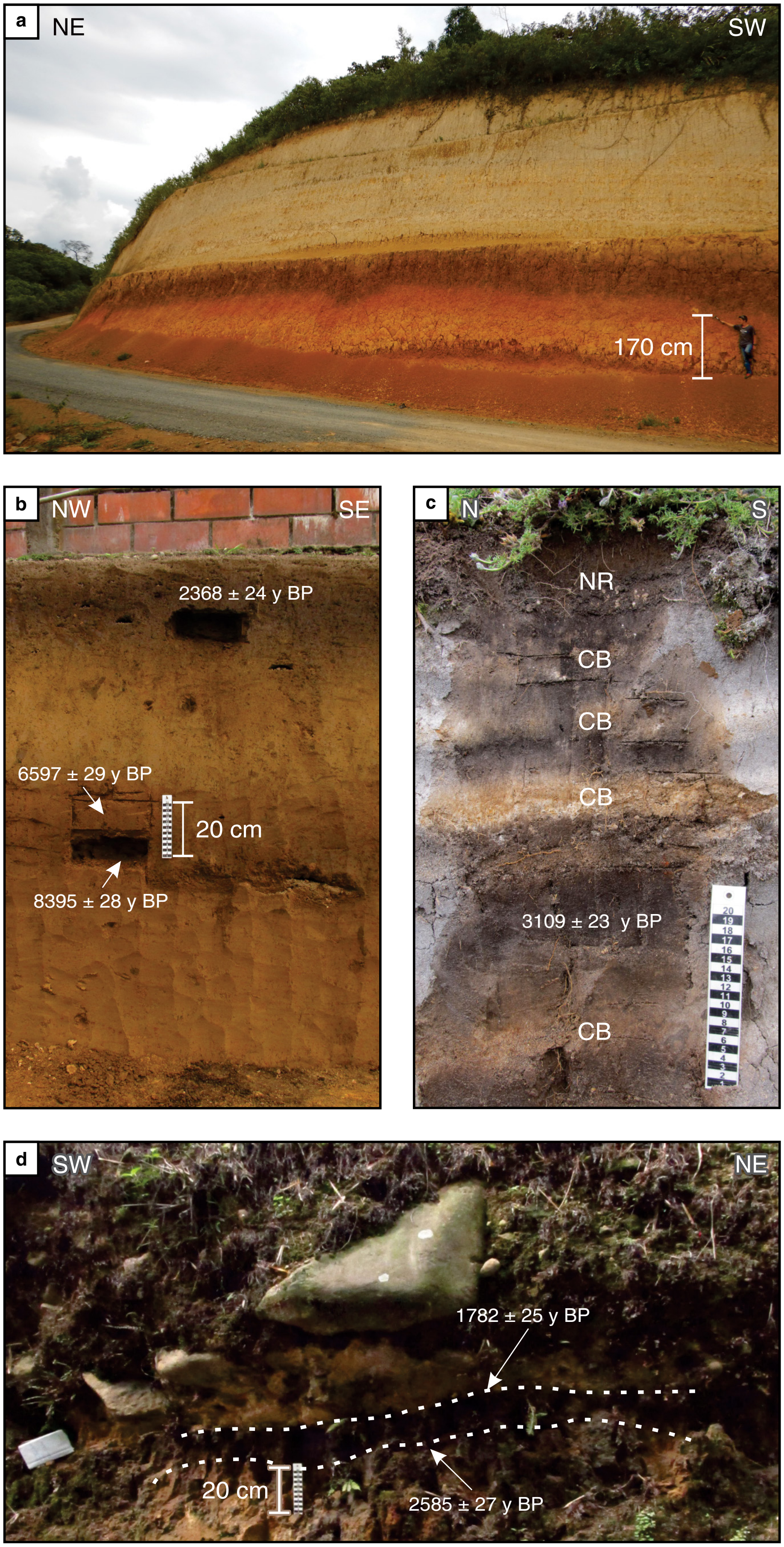
a
NE
SW
170 cm
b
NW
SE
2368 ± 24 y BP
6597 ± 29 y BP
20 cm
8395 ± 28 y BP
c
N
S
NR
CB
CB
CB
3109 ± 23 y BP
CB
d
SW
NE
1782 ± 25 y BP
20 cm
2585 ± 27 y BP

←

Figure 9. Outcrop photographs of the Potreros–Porvenir–El Roble Formation and overlying holocenic pyroclastic fallout associated with exogenous lithosomes in the study area. **(a)** General view of the pyroclastic successions in the Conjunto Residencial San José locality (Pereira city). **(b)** Tephra layers separated by a paleosol (and their ^{14}C ages) in the Marsella sector. **(c)** Succession of tephra layers related to the activity of the Nevado del Ruiz (NR) and Cerro Bravo (CB) Volcanoes and interbedded paleosols (and ^{14}C ages). **(d)** Interlayered epiclastic deposits and fallout pyroclastic layers separated by a paleosol (and ^{14}C ages). Scales in cm.

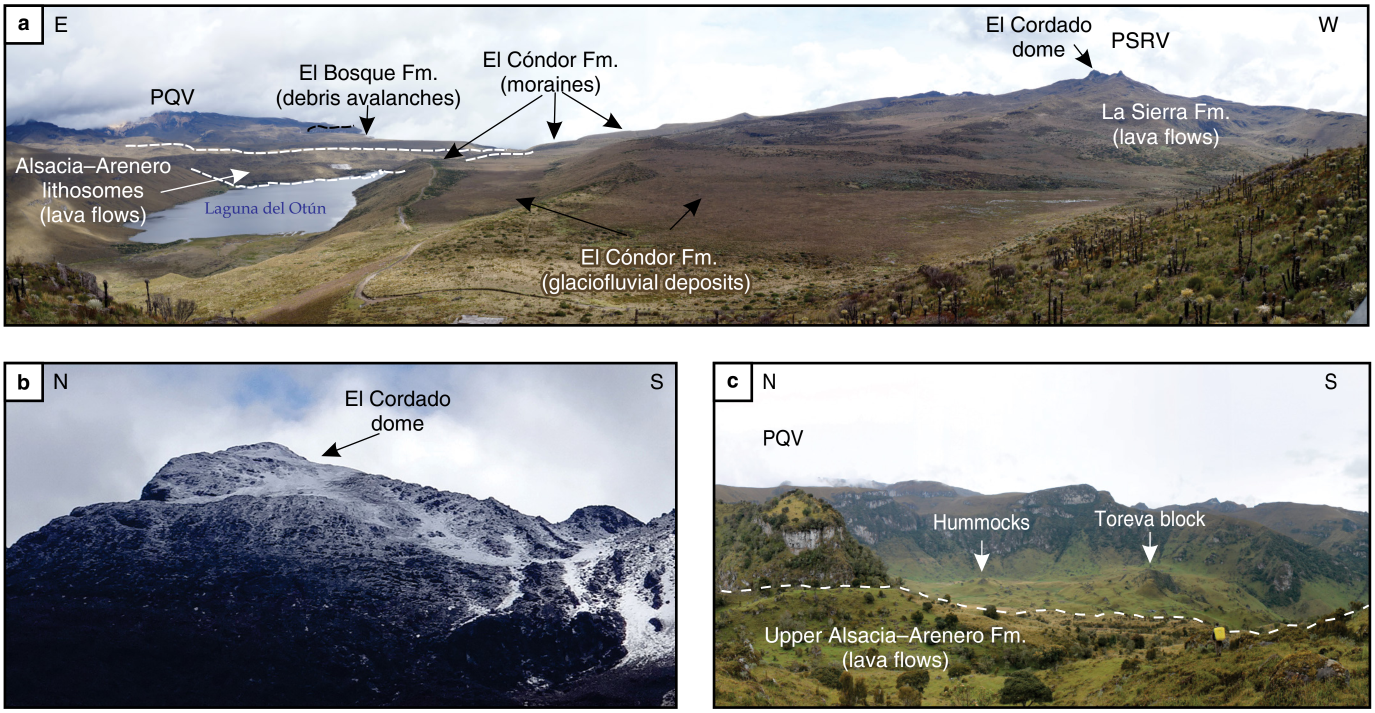

Figure 10. Panoramic view of the PSRV and PQV. **(a)** N and E localities of the PSRV summit showing the main geomorphological features and lithostratigraphic units. **(b)** Close view of El Cordado dome. **(c)** Collapse amphitheater cutting the NW flank of the PQV, together with the hummocks on the surface of the corresponding debris avalanche deposits of El Bosque Formation. (Fm.) Formation.

hummocks and small shallow lakes. The collapse amphitheater affecting the PQV has almost vertical 300 m–high walls and a maximum diameter of 2.14 km (Figure 10c).

Locally, holocenic deposits of pyroclastic fallout cover proximal and distal portions of the PSRVC and the pyroclastic layers of the Potreros–Porvenir–El Roble Formation. They are generally characterized by thin to medium layers, light tan and pinkish yellow colors, and tabular geometry, with variations in grain size from medium lapilli to fine ash. Some paleosol layers are interbedded with these pyroclastic layers, which are up to 40 cm thick and contain archaeological fragments (lithofacts) and paleosols (Figure 9b, 9c, 9d) in which several AMS ^{14}C ages have been obtained at 8395 ± 28 years BP (stable fraction), 6597 ± 29 years BP (labile fraction), 5198 ± 30 years BP (stable fraction), and 3109 ± 23 years BP (stable fraction).

The Valle Largo Formation (Figure 11a, 11b) crops out in the E and NE areas of the PSRV and is well exposed along the trail from Potosí to El Bosque. It consists of concentrated and dilute PDCs overlaid by pyroclastic falls (Figure 11a, 11b). The concentrated PDC deposit is massive, poorly sorted, and matrix–supported, with a visible thickness >1 m; it is also monolithologic and dominated by angular porphyritic lava fragments embedded in a crystal–lithic ash matrix. The dilute PDCs reach up to 2 m in total thickness with thin layers and laminae and consist of moderate to well–sorted lapilli tuffs composed of angular lithic fragments of medium porphyritic, gray and red lavas and pumice lapilli (pumice in the upper portion only) embedded in a matrix of fine to coarse ash; they exhibit parallel to wavy lamination beds as well as lenses of lapilli. These PDC deposits are overlain by an ash fall layer 6 to 60 cm thick that is clast–supported, well–sorted, and composed of angular to subangular medium pumice lapilli and accessory lava lithic fragments. On this layer, a paleosol is developed, up to 40 cm in thickness and dated by AMS ^{14}C on the stable fractions of organic matter at 7192 ± 38 and 7152 ± 29 years BP. Above the paleosol, there are ash–rich deposits from presumably dilute PDCs (Figure 11a, 11b, 11c) of the Otún Formation that crop out in the E areas of PSRV that reached a maximum thickness of 60 cm in the laguna del Otún locality. This material consists of weathered laminated to thin layered deposits that are ma-

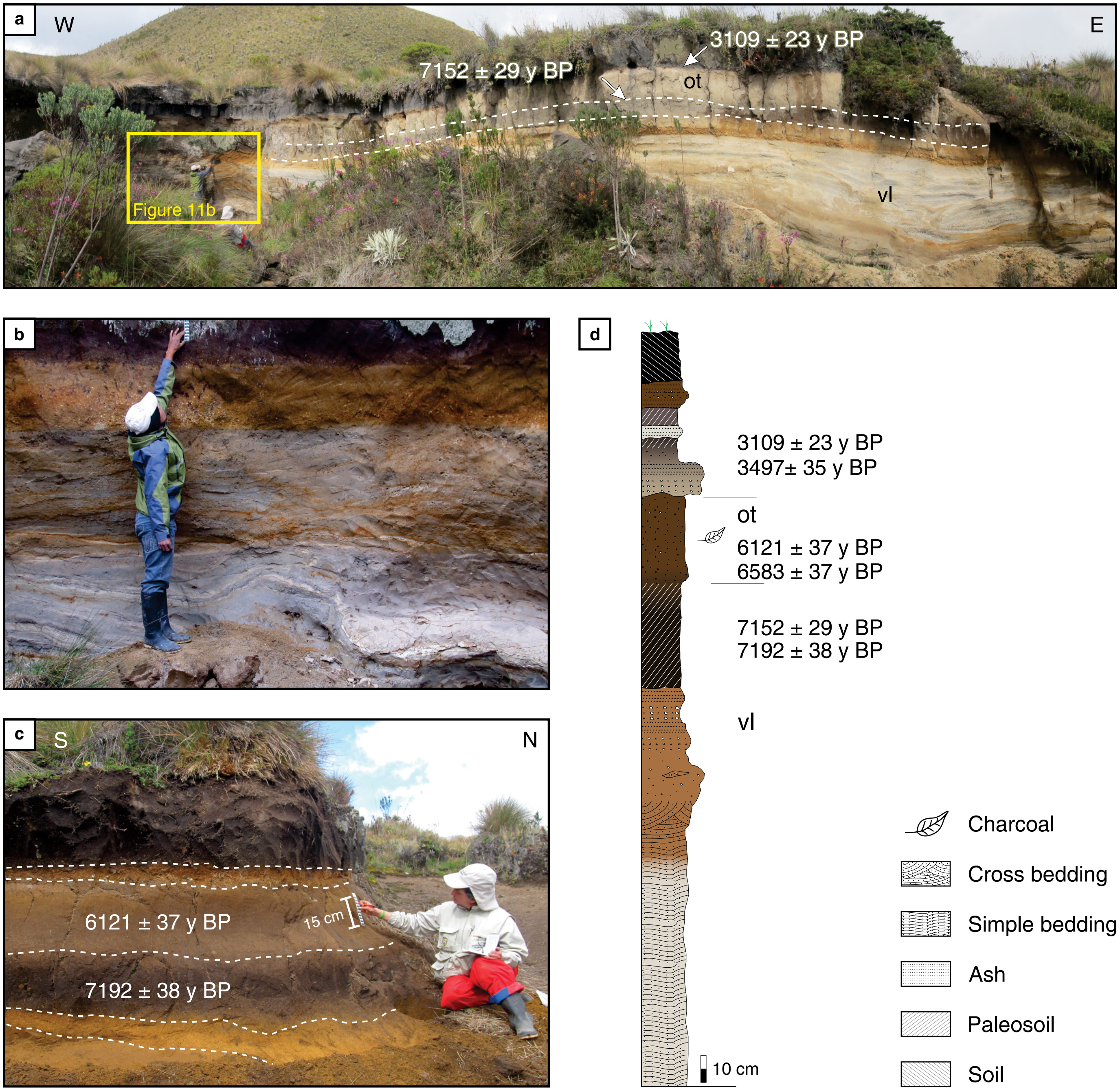

Figure 11. Outcrop photographs and schematic stratigraphic section of the Valle Largo (vl) and Otún (ot) Formations in the SE area of the PSRV. **(a)** Panoramic view of the main outcrop that shows the thickness variations and facies of the two units, separated by a paleosol. **(b)** Detail of the outcrop, showing the massive to stratified gray to ochre deposits of the Valle Largo Formation. **(c)** Along the laguna del Otún–El Bosque pathway, the Valle Largo and Otún Formations together with the crop out. The ^{14}C age of 6121 ± 37 years BP corresponds to the Otún Formation and 7192 ± 38 years BP to the paleosol of the Valle Largo Formation. **(d)** Representative stratigraphic column of the NE, E, and SEE localities of the PSRV. For the eruptive history and conventions, refer to Figure 4.

trix–supported and well–sorted, composed dominantly of ash with crystals (plagioclase, amphibole, and pyroxene), sparse fine lapilli of lava and pumice (the latter proportion is lower) and containing mm–sized charcoal fragments, which yield AMS ^{14}C ages of 6121 ± 37 years BP (Figure 11c) and 6583 ± 37 years BP.

On the summit of the PSRV, El Cordado unit is located and is composed of a coulée–lava dome emplaced to the NW of PSRV, near the headwaters of Los Pájaros and San Ramón streams (Figure 10a, 10b). This dome has ogives on the surface, it is 0.54 km long, 0.30 km wide, and 150 m thick and is characterized by a lack of glacial sculpting. Dense vegetation and steep topography cause limited access to the summit portion of the study area, so we cannot provide more detailed information about the dome and its composition. However, given its morphology, we think that the dome could be of andesitic to dacitic composition.

In the eastern side of the PSRV, lava flow units of the Lower and Upper Alsacia–Arenero Formations are representative of external volcanic sources (external lithesome; Figures 2d, 10a). Pyroclastic fall deposits of the Valle Largo Formation cover the Lower Alsacia–Arenero Formation, which comprises lava emplacements topographically lower and differently oriented than those of the Upper Alsacia–Arenero Formation. Lava flows of the Lower Alsacia–Arenero Formation are andesitic blocky lavas forming dissected lobes up to 1.8 km long and 30 m thick that show ogives on the surface. The Upper Alsacia–Arenero Formation is represented by andesitic blocky–lava flows (61.17 wt % SiO_2) up to 70 m thick and 12 km long, which also exhibit ogives on the surface. They crop out along the Otún River basin to the south and reach Peña Bonita place at an elevation of 2550 masl.

Fluvial–lacustrine deposits of the El Mosquito Formation are recognized in the area of lagunas Otún, Maria Pardo, and El Mosquito, corresponding to thin beds of silts and sands interbedded with light brown peats dated by AMS ^{14}C at 4666 ± 36 and 4962 ± 36 years BP.

A series of mapped terraces up to 15 m thick is defined as epiclastic deposits of the Matecaña and Guacas Formations, interbedded with pyroclastic fallout deposits and a paleosol with ages of 1782 ± 25 years BP (labile fractions) and 2585 ± 27 years BP (stable fractions) (Figure 9d). Their epiclastic deposits are massive, matrix–supported, locally reversely graded, and poorly sorted; they predominantly contain subrounded to rounded volcanic blocks and gravels, as well as metamorphic and plutonic rock fragments within a silty–sandy matrix. These deposits are identifiable at the following localities: in the middle basin of the Otún River, the Parque Industrial de Pereira, the Pereira–Dosquebradas highway, La Romelia–El Pollo road, the middle basin of the San Eugenio River, El Vergel neighborhood (nearby the main road between Manizales and Pereira), and in La Coca locality (La María–El Español road).

5. Discussion

5.1. Structural Framework

The proximal and middle zones of the PSRVC are affected by the southern end of the Palestina Fault System, whose segments, including the Santa Rosa Fault, exhibit a predominant NE–SW trend. These fault system segments widely affect the volcanic deposits of the PSRVC and control the upper portion of the Otún River basin (López, 2014) and the possible emplacement of magmas within the volcanic complex. Another important fault system corresponds to a series of NW–SE structures (Central Hidroeléctrica de Caldas, 1983; Thouret, 1988) that control the channels of the Campoalegre, San Ramón, Campo Alegrito, and San Eugenio Rivers, and La Cristalina stream. The W area of the PSRVC proximal zone is affected by the San Jerónimo and Manizales Faults along a predominantly N–S trend. The San Vicente and Santa Rosa thermal springs (Central Hidroeléctrica de Caldas, 1983) are presumably controlled by the intersection of NW–SE with N–S to NNE–SSW and NE–SW faults.

According to the analyzed structural information available in the geological literature and from the field work and remote sensing carried out in the area, in the PSRVC distal zone, specifically in the Quindío–Risaralda Fan, there are fault systems (Bohórquez et al., 2005; Espinosa, 2015; Guarín, 2008; Lalinde, 2004; Neuwerth, 2009; París et al., 2000; Suter, 2008) oriented N–S, which are related to the Cauca–Romeral Fault System (San Jerónimo, Silvia–Pijao, and Cauca–Almaguer Faults, among other local faults; Figure 3a). NW–SE structures correspond to transcurrent and transtensive systems with important segments such as the Otún and Consota Faults. The transcurrent kinematics of the faults that make up the Cauca–Romeral System have produced traction (pull–apart) basins, which possibly generated depositional spaces for the emplacement of the Quindío–Risaralda Fan. These spaces are filled with volcaniclastic, epiclastic, and alluvial deposits. The recent tectonic activity of the fault systems in the distal part of the PSRVC, specifically in the Quindío–Risaralda Fan area, has produced tectonic blocks, the dynamics of which locally change existing drainage patterns. Erosional–depositional processes have remobilized existing volcaniclastic and pyroclastic fallout deposits, thus configuring new and local geoforms that partially modify the general morphology of the volcaniclastic Quindío–Risaralda Fan.

5.2. Geological Evolution and Eruptive History

Stratigraphical and geomorphological field work and geological mapping supported by isotopic ages, together with petrographical and geochemical data, lead us to interpret the main features of the geological evolution and eruptive history of the PSRVC. An age range of two eruptive periods and six epochs are established, considering intervals of volcanic activity and inactivity (Figure 12).

The first eruptive period was characterized by the building up of the Pre–PSRV. This volcano is largely eroded and dismantled, but its remnants provide evidence of intense effusive activity (Eruptive epoch 1.1; Figure 12a) that produced a succession of andesitic and dacitic lava flow units (Tarapacá Formation) dated at 2.3 ± 0.1 Ma (Thouret, 1988). The longest lava emplacement (ca. 25 km) of this ancient volcano is a very uncommon case for these kinds of compositions, since they rarely reach lengths >15 km (Kilburn, 2000). Another similar case

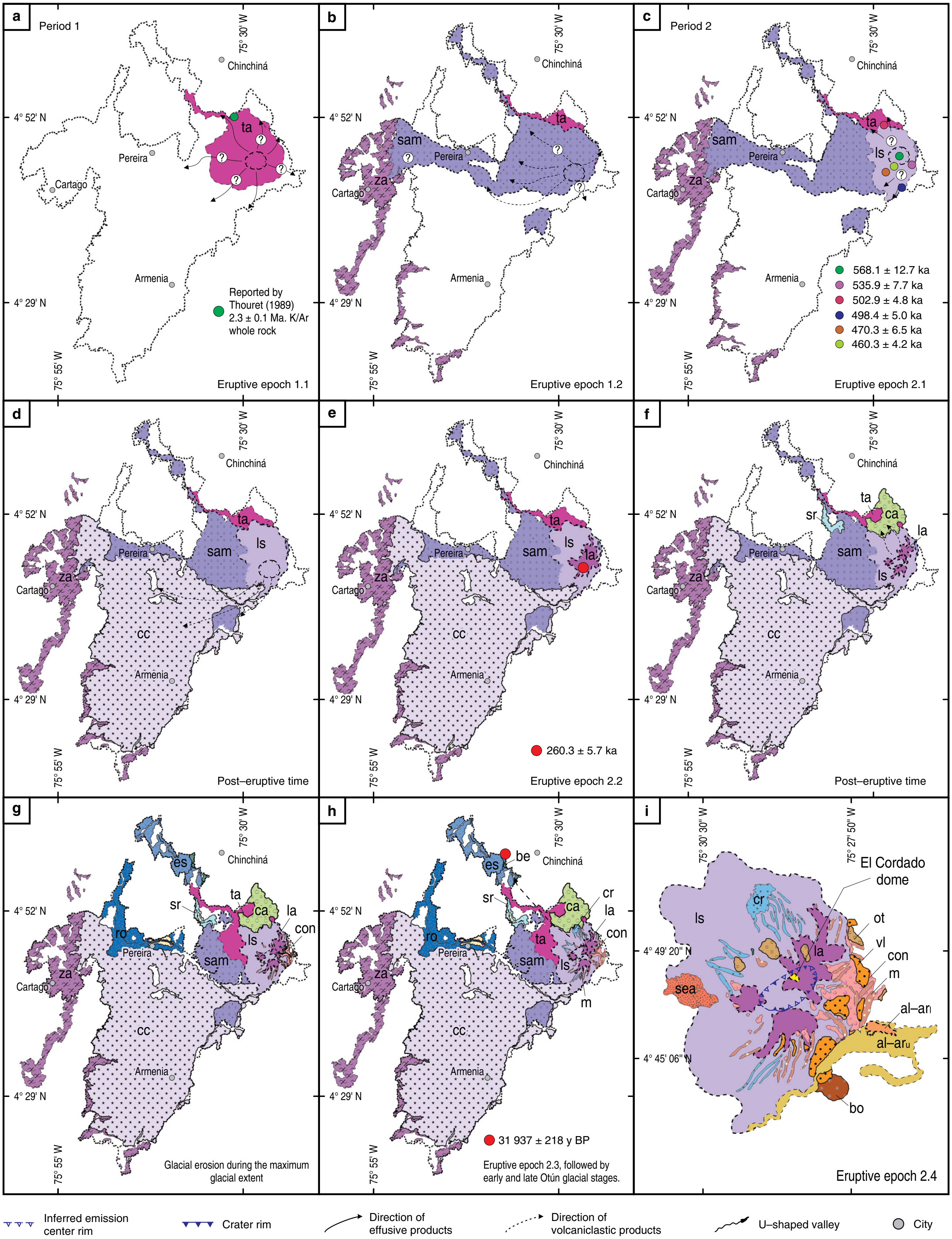
a
Period 1
75° 30' W
Chinchiná
4° 52' N
ta
Pereira
Cartago
Armenia
4° 29' N
Reported by
Thouret (1989)
2.3 ± 0.1 Ma. K/Ar
whole rock
75° 55' W
Eruptive epoch 1.1
b
sam
za
Eruptive epoch 1.2
c
Period 2
ls
568.1 ± 12.7 ka
535.9 ± 7.7 ka
502.9 ± 4.8 ka
498.4 ± 5.0 ka
470.3 ± 6.5 ka
460.3 ± 4.2 ka
Eruptive epoch 2.1
d
cc
Post–eruptive time
e
la
260.3 ± 5.7 ka
Eruptive epoch 2.2
f
sr
ca
Post–eruptive time
g
es
ro
con
Glacial erosion during the maximum
glacial extent
h
be
cr
m
31 937 ± 218 y BP
Eruptive epoch 2.3, followed by
early and late Otún glacial stages.
i
75° 30' 30" W
75° 27' 50" W
El Cordado
dome
ot
vl
4° 49' 20" N
4° 45' 06" N
sea
al–ar
bo
Eruptive epoch 2.4
Inferred emission
center rim
Crater rim
Direction of
effusive products
Direction of
volcaniclastic products
U–shaped valley
City

Figure 12. Chronostratigraphic sketch of the main stages of the geological evolution and eruptive history of the PSRVC showing the distribution of the deposits formed in each epoch or in posteruptive and prolonged quiescence interval. For the eruptive history and conventions, refer to Figure 4.

is reported by Martínez et al. (2014) in the Nevado del Ruiz Volcanic Complex, where an andesitic lava flow reached ca. 30 km long (El Líbano lava flow). According to Walker (1973), the factors governing the length of the lava extrusion are the initial viscosity of the lava, the total volume of lava extruded, the rate of effusion, the slope of the underlying surface, the form of the topography, and some other special cases in which the lava flows entirely on land or enters the water. For the lava of the Pre–PSRV case (and perhaps for some lava of the Nevado del Ruiz Volcanic Complex), further research may solve the lava length problem but we suspect that some special variations in the control factors cited by Walker (1973) should have occurred to favor such exceptional lengths. Hence, further studies should be focused on trying to solve these particular cases.

The Eruptive epoch 1.2 (Figure 12b) was characterized by explosive eruptions, and PDC deposition (Samaria Formation) extended mainly towards the W and SW from the PSRVC. In Cartago, La Virginia, Puerto Alejandría (Quimbaya), and Puerto Samaria (Montenegro) localities and SE of La Tebaida, we interpret fluvial and lacustrine deposits intercalated with volcaniclastic deposits as successive eruptions separated by intervals of repose, possibly, associated with the transformation of concentrated PDCs of the Samaria Formation that caused channel damming and modifications to the accumulation patterns of the sediments. This inter–eruption process lasted approximately between 2.05 ± 0.60 and 0.79 ± 0.22 Ma according to $^{40}Ar/^{39}Ar$ data in biotites performed by Neuwerth (2009). The succession in this zone has been mapped regionally as the Zarzal Formation, originally described as formed by fine–grained lacustrine sediments with the presence of diatomites alternating with sands and gravels of fluvial domain and volcanic mass flows coming from the Central Cordillera (Suter, 2008). The posteruptive interval was characterized by the generation of lahars that reworked the previous pyroclastic deposits (upper portion of the Samaria Formation). Then, a prolonged period followed, characterized by glacial, glacial–fluvial, fluvial, and denudation processes that favored the generation of thick epiclastic deposits.

The second eruptive period corresponds to the development of the main PSRV. Its early activity (Eruptive epoch 2.1) produced andesitic and dacitic lava flow units (La Sierra Formation) from an old emission center in the area of the previous Pre–PSRV summit volcano (Figure 12c). These lava flows have $^{40}Ar/^{39}Ar$ ages between 568 ka and 460 ka. The posteruptive time interval (Figure 12d) was characterized by debri avalanches from the gravitational collapse of the S–SW flanks of the PSRV and subsequent lahars (Cedral–Ceilán Formation). The corresponding deposits filled wide paleobasins within the present–day Departments of Risaralda, Quindío, and northern Valle del Cauca. They contain fragments related to lithologies that also suggest the pre–existence of domes in the summit area of the PSRV. These deposits have been subjected to intense weathering, erosion, and reworking processes. This study considers that a very large portion of the deposits of the Quindío–Risaralda Fan correspond to debris avalanche, lahars, and epiclastic deposits and that the morphology of the area has been covered by external fallout deposits and has been strongly influenced by fluvial, tectonic, and erosive dynamics that especially affected the upper fan deposits.

The debris avalanche deposits of the Cedral–Ceilán Formation, recognized initially in the middle portion of the Otún River basin, can be related to those described in the same locality by Corporación Autónoma Regional de Risaralda & Haskoning (1986) as "lithified pyroclastic flow of the middle Quaternary". These authors consider them as belonging to a single flow or a sequence of very thick pyroclastic flows containing semi–rounded volcanic clasts in a highly lithified sandy matrix that come from the main crater of the PSRV or on its flank in a source currently hidden by glacial deposits. These authors mention that this flow apparently filled the contemporaneous valley of the Otún River, creating a surface as much as 70 m below the surface of the Quindío–Risaralda Fan along the river canyon. This unit can also be related to what Espinosa (2000) and Espinosa–Baquero (2020) call "Old Quaternary", essentially corresponding to mass flow deposits (debris avalanches and lahars), among which the author highlights three major geomorphological groups (proximal, intermediate, and distal fans), possibly related to different phases of tectonism, volcanism, and climate change. Several deposits of the Cedral–Ceilán Formation are associated with what Guarín (2008) called the "Quindío–Risaralda Fan". The author subdivided the deposits into 45 depositional units from debris avalanches and hyperconcentrated flows, resulting from the interaction between ice layers and volcanic activity of the Cerro Bravo–Cerro Machín volcanic massif, as well as from the destruction of volcanic cones involved in its evolution.

After the S–SW–dipping flank collapses and the subsequent interval of quiescence and erosion, the PSRV resumed its activity (Figure 12e), and effusive eruptions that produced a thick succession of andesitic and dacitic lavas cropping out in the proximal zone (Las Águilas Formation). This eruptive epoch is $^{40}Ar/^{39}Ar$ dated at 260.3 ± 5.7 ka.

The posteruption time (Figure 12f) was characterized by partial gravitational collapses that destroyed part of the W flank of the stratovolcano, which generated debris avalanches (Campoalegre Formation) distributed to the NW in the sectors of the Campoalegre and Campo Alegrito River basins and La Cristalina stream. Subsequent lahar deposits of the Santa Rosa Formation were emplaced along the San Eugenio River and La Leona stream.

After the collapse, a prolonged quiescence interval in volcanic activity was characterized by intense glacial erosion and reworking during the maximum glacial extent in Colombia, which occurred in the study area (Figure 12g) between 48 and 28 ka (Thouret et al., 1997). Alternatively, according to van der Hammen (1985), it could have occurred before 35 ka or 45–25 ka (as shown in Figure 2 of van der Hammen, 1985). Thick glacial and glacial–fluvial deposits and moraines were formed (La Cristalina unit). Moreover, this long interval of volcanic inactivity was characterized by processes of erosion and dismantling that generated thick accumulations of epiclastic deposits that partially filled the Otún, Campoalegre, and San Eugenio Rivers basins (La Romelia–El Pollo and La Esmeralda Formations) in the distal zone of the PSRVC in the municipalities of Santa Rosa de Cabal, Dosquebradas, and Pereira. Several of these deposits were possibly fed by melt water from the glacial mass corresponding to the peak of the maximum glacial extent of the last glaciation.

Intense explosive activity from neighboring eruptive sources produced a thick accumulation of fallout deposits (Potreros–Porvenir–El Roble Formation) dated between 45 709 ± 1326 and 22 812 ± 84 years BP (Table 2). The high degrees of alteration and weathering preclude a good characterization of these deposits. According to Toro & Hermelín (1991), there is a regional assemblage of ash layers that are rich in amphibole crystals, which they called an "Assemblage of ancient ashes" that are older than 10 000 years, on which newer ash layers were deposited. Although all of these ash layers are considered deposits of pyroclastic falls in this work, it cannot be excluded that many of the ash layers that cover the medial and distal parts of PSRVC and that are part of the upper portion of the Quindío–Risaralda Fan correspond to PDCs, which could have reached greater distances. This theory is based on the variation in thickness presented in some of them for which the continuity could be followed as far as close to La Vieja River (western end of the Quindío–Risaralda Fan), where thicknesses up to 1 m are recorded, contrasting with their nondeposition in the serranía de Santa Bárbara to the western side of La Vieja River. The high levels of alteration and weathering in all of these layers preclude good characterization and correlation. Therefore, more detailed studies about the characterization and provenance of these deposits are strongly recommended.

A new explosive eruption occurred at 31 937 ± 218 years BP (Figure 12h) and produced PDC deposits emplaced towards the Campo Alegrito and Campoalegre Rivers basins (Betania Formation); its distal facies deposits suggest that they were transformed to lahars.

At the end of the Pleistocene and beginning of the Holocene (Figure 12h), the glacial processes associated with the early and late Otún glacial stages occurred at 13.5–10.5 ka (Thouret & van der Hammen, 1981) generated glacial and glacial–fluvial deposits (El Cóndor Formation) along with strong erosion and reshaping of the previous volcanic edifice and its products.

Following these glacial stages, gravitational collapses affected the W and SW flanks of the PSRV and generated thick debris avalanche deposits (Los Alpes Formation and San Eugenio Alto unit). These deposits are presumably stratigraphically coeval with the debris avalanche deposit generated by the massive landslide in the NW flank of the PQV (El Bosque Formation). These contemporaneous events could have been facilitated by significant seismic activity in the area, as similarly was reported by Martínez et al. (2014) in the Nevado del Ruiz Volcanic Complex.

The Holocene activity of the PSRV (Figure 12i) is dated at 7 to 6 ka and was intensely explosive, generating concentrated PDCs and evolving into more explosive eruptions that produced dilute pumice–bearing PDCs, with some associated pumice pyroclastic fallout layers (Valle Largo and Otún Formations) emplaced to the E and NE of the study area. These eruptions are considered the maximum expected eruptive events for hazard evaluation in this area. PDCs were possibly associated with events involving disruption of summit domes due to recharging or injection into the magmatic system.

Possibly during or close to the occurrence of this activity, the emission of the coulée–lava dome El Cordado occurred at the summit of the PSRV. Given difficult access to the area, it was not possible to obtain detailed information about the lithology of the dome and its composition, as well, the stratigraphic features that provide a relative age for its emplacement was not achieved; nevertheless, the lack of glacial sculpting and the well–preserved surface of the dome suggest that this emplacement could be considered as recent as the Holocene; together with the Valle Largo and Otún Formations, it represents the last magmatic recharge recorded in the PSRV.

Alternating effusive activity from an external volcanic source to the E produced distinct lava flow units (Lower and Upper Alsacia–Arenero Formations). These lavas are interpreted to have recurrently induced damming of the Otún River, consequently forming the laguna del Otún. This process occurred in two episodes. The initial episode occurred at approximately 7200 years BP, and the second episode occurred slightly more than 4962 ± 36 years BP, when the lagunas María Pardo and El Mosquito were also formed. Thinly bedded fluvial–lacustrine silts and sands interbedded with light brown peats (El Mosquito Formation) indicate repose times in volcanic activity in the study area. Additionally, pyroclastic fallout from an external volcanic source produced a widespread accumulation of ash deposits that covers the distal parts of the PSRVC. These deposits crop out in the sectors of Cocora, Chagualá, and Circasia (Quindío), as well as in Pereira and Marsella, Risaralda, and are dated between 8395 ± 28 and 5198 ± 30 years BP (Table 2).

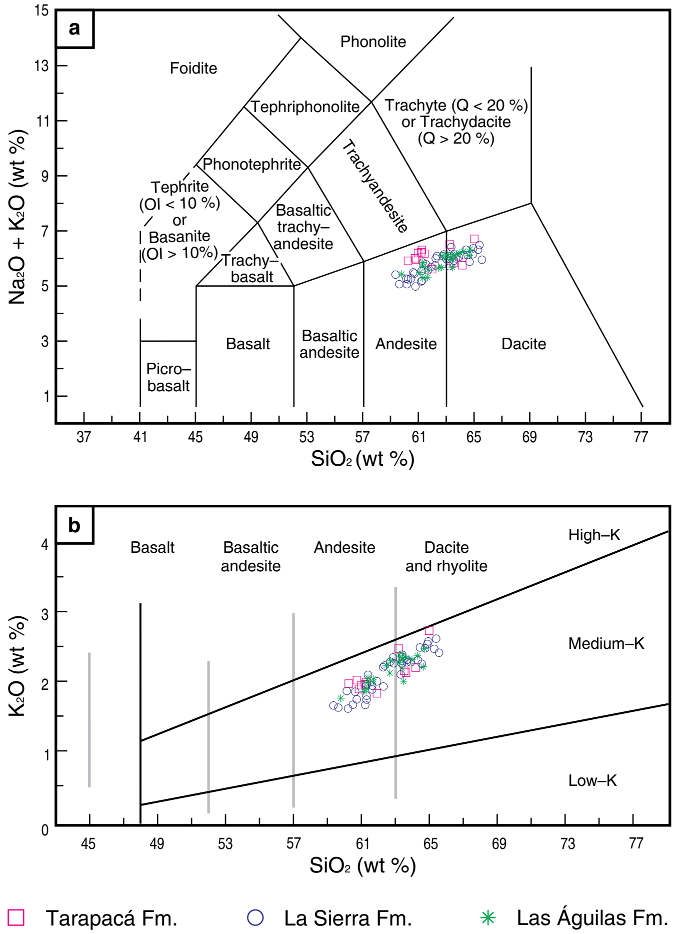

Figure 13. Geochemical behavior of PSRVC lavas. **(a)** Chemical classification of volcanic rocks according to Le Maitre (2002) based on total alkalis versus silica (TAS). **(b)** SiO_2 vs. K_2O diagram of Le Maitre (2002). Fm: Formation.

Further explosive activity from external volcanic sources corresponding to the Cerro Bravo, Nevado del Ruiz, Cerro Machín, and Tolima Volcanoes produced plinian and subplinian fallout deposits dated at less than 3497 ± 35 years BP that widely cover proximal parts of the study area.

The posteruptive activity continued after 1782 ± 25 years BP with local emplacements of epiclastic deposits in the Otún and San Eugenio Rivers basins (Matecaña and Guacas Formations).

Additionally, the geochemical data obtained in samples from the PSRVC come from mainly effusive products (see Correa et al., 2017), as shown in Figure 13, which represent the most important inputs of magma that built up this volcanic complex; nevertheless, new geochemical studies should also be focused on pyroclastic products to allow comparison and association of both effusive and explosive magmatic products. Such studies could also allow us to investigate the magmatic evolution of the complex, including the Holocene magmatic products.

6. Conclusions

Starting from lithostratigraphic and geomorphological field work together with geological mapping supported by new isotopic ages and petrographic and geochemical data, the geological evolution and eruptive history of the PSRVC were established by integrating the use of lithostratigraphic units (for mapping), lithosomes (for defining eruptive centers), unconformities (for defining erosive or nondepositional surfaces), and volcanic activity units (for the main steps of the eruptive history). Accordingly, we described an eruptive history characterized by two eruptive periods corresponding to the construction of the Pre–PSRV (at 2.3 Ma) and the PSRV (between 568 ka and the Holocene). The earlier stage comprised two eruptive epochs, including effusive and explosive activity as well as quiescence intervals. The later stage was characterized by four eruptive epochs organized into a series of effusive and minor explosive eruptions interrupted by a number of gravitational collapses that generated debris avalanche and lahar deposits, and punctuated by intense glacial reshaping and intense erosion, which produced thick accumulations of glacial and glacial–fluvial deposits in the parts of the volcano at higher elevations and thick epiclastic deposits within the river valleys. The Holocene activity of PSRV (7–6 ka) was mostly explosive with the generation of repeated PDC deposits and minor fallout, probably, associated with repeated explosions of summit domes; evidence of effusive activity is provided by the currently noted emplacement of a coulée–lava dome at the summit of PSRV, which together with the explosive activity mentioned represent the latest eruptions of this volcano; these episodes must be considered in hazard assessment.

To clarify the relationship of the PSRVC deposits with those of adjacent volcanic sources and to contribute to the knowledge of the stratigraphy of the area, we partially mapped and dated external lithosomes at different stratigraphic positions interlayered with or covering those of the PSRVC, thus documenting the evidence of their contemporaneous or alternating eruptive activity or inactivity. We characterized deposits of external lithosomes from the San Diego–Cerro Machín Volcano–Tectonic Province (pyroclastic successions of fallout deposits), Alsacia–Arenero Volcanoes (blocky lava emplacements), and PQV (debris avalanche deposits).

The presence of the PSRVC in the study area is linked to an active extensional tectonic regime along dominant NE–SW–trending fault systems (mainly the Palestina Fault) and NW–SE–trending fault systems; therefore, recorded flank collapses that have occurred through the history of the PSRVC and in its vicinity could be related to the interactions of both fault systems and local conditions.

The range in chemical composition of PSRVC varies between andesitic and dacitic units (59.33 to 65.52 wt % SiO_2) of calc–alkaline affinity, with moderate K_2O contents (1.47–2.75 wt %). Petrographically, the PSRVC products have wide textural variations with poor mineralogical variation.

Acknowledgments

The present study was supported by the Colombian government through the Servicio Geológico Colombiano within the "Proyecto Ampliación del conocimiento geológico y del potencial de recursos del subsuelo de la nación (Extension of geological knowledge and potential subsoil resources of the nation Project)". The authors of this work acknowledge Luis Jerónimo VALENCIA for his work, commitment, and dedication in all stages of the project and Liliana NARVÁEZ and Diego Fernando PALECHOR, who were part of the technical team in its different stages. Likewise, Natalia PARDO, Silvia Camila CASTILLA, and Maria Fernanda ALMANZA are acknowledged for providing excellent discussions. Thanks are also extended to the inhabitants of the páramo lands and the high mountains of the Paramillo de Santa Rosa, especially those who accompanied the geologists during the long field days; likewise, thanks are given to the authorities of the Santa Rosa de Cabal, Pereira, Dosquebradas, Marsella, and La Virginia (Risaralda Department); Armenia, Calarcá, La Tebaida, Montenegro, Quimbaya, Circasia, Filandia, and Salento (Quindío Department); and Cartago, Caicedonia, Alcalá, Obando, and Ulloa (Valle del Cauca Department). Thanks are also extended to the following entities and governmental and private institutions for their collaboration and information provided during the project: the Corporación Autónoma Regional de Risaralda, Parque Nacional Natural Los Nevados, Aguas y Aguas de Pereira, Santuario de Fauna y Flora Otún–Quimbaya, Consejo Municipal de Gestión del Riesgo of Santa Rosa de Cabal, Risaralda Disaster Risk Management Council, Community Federation for the Management and Regulation of Risaralda Protected Areas, and the Disaster Prevention and Attention, Operations Management. Thanks to Gloria Patricia CORTÉS and Adriana AGUDELO from the Observatorios Volcanológicos y Sismológicos de Manizales and Popayán and all their technical and operational staff. To the Servicio Geológico Colombiano management of the Dirección de Geociencias Básicas, which was led by geologist Alberto OCHOA and currently by Mario CUÉLLAR, and to the Servicio Geológico Colombiano Dirección de Laboratorios led by Héctor ENCISO and currently by Hernando Alberto CAMARGO–GARCÍA. Finally, we thank the reviewers Federico LUCCHI (Universitá di Bologna) and Jhon Jairo SÁNCHEZ (Universidad Nacional de Colombia) for the very important and time–consuming comments, ideas, suggestions, and corrections, which helped enormously to improve this manuscript.

References

Alfaro, C., Aguirre, A. & Jaramillo, L.F. 2002. Inventario de fuentes termales en el Parque Nacional Natural de los Nevados. Ingeominas, unpublished report, 101 p. Bogotá.

Bohórquez, O.P., Monsalve, M.L., Velandia, F., Gil, F. & Mora, H. 2005. Marco tectónico de la cadena volcánica más septentrional de la cordillera Central de Colombia. Boletín de Geología, 27(1): 55–79.

Boussingault, J.B. 1892–1903. Mémoires de Jean Baptiste Boussingault. 5 volumes. Chamerot & Renovard. París, France.

Caballero, H. & Zapata, G. 1984. Geología de la plancha 224 Pereira. Scale 1:100 000. Ingeominas. Bogotá.

Cardona, J.F. & Ortiz, M. 1994. Aspectos estratigráficos de las unidades del intervalo Plioceno – Holoceno entre Pereira y Cartago. Propuesta de definición para la Formación Pereira. Bachelor thesis, Universidad de Caldas, 124 p. Manizales, Colombia.

Central Hidroeléctrica de Caldas S.A. 1983. Investigación geotérmica Macizo Volcánico del Ruiz: Fase II, Etapa A, Geovolcanología, III, 228 p. Manizales.

Chang, K.H. 1975. Unconformity–bounded stratigraphic units. GSA. Bulletin, 86(11): 1544–1552. https://doi.org/10.1130/0016-7606(1975)86<1544:USU>2.0.CO;2

Consiglio Nazionale delle Richerche Commissione per la Cartografia Geologica e Geomorfologica. 1992. Carta geológica d'Italia 1:50 000. Guida al rilevamento. Servizio Geologico Nazionale, Quaderni, Serie III, 1, 11p. Istituto Poligrafico e Zecca dello Stato. Roma, Italy.

Corporación Autónoma Regional de Risaralda & Haskoning. 1986. Plan de ordenamiento, prevención de desastres y saneamiento ambiental del rio Otún. Zonificación de riesgos, II. Hidrología, p, 57–113. Pereira, Colombia.

Correa, A.M., Cruz, Y.P., Pulgarín, B.A., Tamayo, M., Valencia, L.G. & Méndez, R.A. 2017. Petrografía y geoquímica de lavas del Complejo Volcánico Paramillo de Santa Rosa (CVPSR). XVI Congreso Colombiano de Geología. Memories, p. 1946–1951. Santa Marta, Colombia.

Duque–Caro, H. 1990. El Bloque Chocó en el noroccidente Suramericano: Implicaciones estructurales, tectonoestratigráficas y paleogeográficas. Boletín Geológico, 31(1): 48–71.

Espinosa, A. 2000. Mapa preliminar de fallas activas del Quindío, zona central. Universidad del Quindío, Proyecto 152, Informe final, 70 p. Armenia, Colombia.

Espinosa, A. 2015. Empalme de las planchas 224 Pereira y 243 Armenia. Modelo geológico, descripción y caracterización de las unidades. El subsistema de Silvia–Pijao. Servicio Geológico Colombiano, unpublished report, 87 p. Bogotá.

Espinosa–Baquero, A. 2020. A model of the Quindío and Risaralda Quaternary deposits. In: Gómez, J. & Pinilla–Pachon, A.O. (editors), The Geology of Colombia, Volume 4 Quaternary. Servicio Geológico Colombiano, Publicaciones Geológicas Especiales 38, p. 333–352. Bogotá. https://doi.org/10.32685/pub.esp.38.2019.09

Estrada, J.J. & Viana, R. 1998. Geología de la plancha 205 Chinchiná. Scale 1:100 000. Ingeominas. Bogotá.

Eusterhues, K., Rumpel, C., Kleber, M. & Kögel–Knabner, I. 2003. Stabilisation of soil organic matter by interactions with minerals as revealed by mineral dissolution and oxidative degradation. Organic Geochemistry, 34(12): 1591–1600. https://doi.org/10.1016/j.orggeochem.2003.08.007

Favilli, F., Egli, M., Brandova, D., Ivy–Ochs, S., Kubik, P.W., Cherubini, P., Mirabella, A., Sartori, G., Giaccai, D. & Haeberli, W. 2009a. Combined use of relative and absolute dating techniques for detecting signals of Alpine landscape evolution during the Late Pleistocene and Early Holocene. Geomorphology, 112 (1–2): 48–66 p. https://doi.org/10.1016/j.geomorph.2009.05.003

Favilli, F., Egli, M., Brandova, D., Ivy–Ochs, S., Kubik, P.W., Maisch, M., Cherubini, P. & Haeberli, W. 2009b. Combination of numerical dating techniques using ^{10}Be in rock boulder and ^{14}C of resilient soil organic matter for reconstructing the chronology of glacial and periglacial processes in a high Alpine catchment during the Late Pleistocene and Early Holocene. Radiocarbon, 51(2): 537–552 p. https://doi.org/10.1017/S0033822200055910

Fisher, R.V. 1966. Rocks composed of volcanic fragments and their classification. Earth–Science Reviews, 1(4): 287–298. https://doi.org/10.1016/0012-8252(66)90010-9

Fisher, R.V. & Schmincke, H.U. 1984. Pyroclastic rocks. Springer–Verlag, 472 p. Berlin, Heidelberg, Germany. https://doi.org/10.1007/978-3-642-74864-6

Gansser, A. 1973. Facts and theories on the Andes. Journal of the Geological Society of London, 129(2): 93–131. https://doi.org/10.1144/gsjgs.129.2.0093

Gómez–Cruz, A.d.J., Moreno–Sánchez, M. & Pardo–Trujillo, A. 1995. Edad y origen del "Complejo Metasedimentario Aranzazu–Manizales" en los alrededores de Manizales (departamento de Caldas, Colombia). Geología Colombiana, 19: 83–93.

Gómez, J., Montes, N.E., Nivia, A. & Diederix, H., compilers. 2015. Mapa Geológico de Colombia 2015. Scale 1:1 000 000. Servicio Geológico Colombiano, 2 sheets. Bogotá. https://doi.org/10.32685/10.143.2015.935

González, H. 1990. Mapa geológico generalizado del departamento de Risaralda. Scale 1:200 000. Ingeominas. Bogotá.

González, H. 1993. Memoria explicativa: Mapa geológico generalizado del departamento de Caldas: Geología y recursos minerales. Scale: 1:250 000. Ingeominas, 62 p. Bogotá.

González, H. & Núñez, A., compilers. 1991. Mapa geológico generalizado del departamento del Quindío. Scale 1:100 000. Ingeominas. Bogotá.

Guarín, F. 2008. Etude sédimentologique du fan volcanoclastique du Quindío–Risaralda (Colombie) et sa relation avec la morphonéotectonique. Doctoral thesis, Université de Genève. 146 p. Genève, Switzerland. https://doi.org/10.13097/archive-ouverte/unige:3960

Helfrich, M., Flessa, H., Mikutta, R., Dreves, A. & Ludwig, B. 2007. Comparison of chemical fractionation methods for isolating stable soil organic carbon pools. European Journal of Soil Science, 58(6): 1316–1329. https://doi.org/10.1111/j.1365-2389.2007.00926.x

Herd, D.G. 1974. Glacial and volcanic geology of the Ruiz–Tolima Volcanic Complex, cordillera Central, Colombia. Doctoral thesis, University of Washington. 77p. Seattle, USA.

Ingram, R.L. 1954. Terminology for the thickness of stratification and parting units in sedimentary rocks. GSA Bulletin, 65(9): 937–938. https://doi.org/10.1130/0016-7606(1954)65[937:TFTTOS]2.0.CO;2

JAXA. 2012. PALSAR User's Guide. 2nd edition. 69 p. https://www.scribd.com/document/208847444/Palsar-User-Guide (consulted in April 2015).

Keith, J.F.J., Rine, J.M. & Sacks, P.E. 1988. Frontier basins of Colombia: Valle del Cauca. University of South Carolina, Earth Sciences and Resources Institute, field report 88–0012, 267 p. Columbia, USA.

Kilburn, C.R.J. 2000. Lava flows and flow fields. In: Sigurdsson, H., Houghton, B., McNutt, S.R., Rymer, H. & Stix, J. (editors), Encyclopedia of Volcanoes. Academic Press, p. 291–305. San Diego, USA.

Kögel–Knabner, I., Guggenberger, G., Kleber, M., Kandeler, E., Kalbitz, K., Scheu, S., Eusterhues, K. & Leinweber, P. 2008. Organo–mineral associations in temperate soils: Integrating biology, mineralogy, and organic matter chemistry. Journal of Plant Nutrition and Soil Science, 171(1): 61–82. https://doi.org/10.1002/jpln.200700048

Kuhry, P. 1988. A paleobotanical and palynological study of Holocene peat from the El Bosque mire, located in a volcanic area of the cordillera Central of Colombia. Review of Palaeobotany and Palynology, 55(1–3): 19–72. https://doi.org/10.1016/0034-6667(88)90053-X

Kuhry, P., Riezebos, P.A., Salomons, J.B. & van der Hammen, T. 1983. Paleoecología de los últimos 6000 años en el área de la laguna de Otún–El Bosque. In: van Der Hammen, T., Pérez–Preciado, A. & Pinto, P. (editors), La cordillera Central colombiana transecto Parque Los Nevados. Estudios de Ecosistemas Tropandinos 1, p. 227–261.

Lalinde, C.P. 2004. Evidencias paleosísmicas en la región Pereira–Armenia, Colombia. Master tesis, Universidad Eafit, 149 p. Medellín, Colombia.

Le Maitre, R.W., editor. 2002. Igneous rocks: A classification and glossary of terms. Cambridge University Press, 263 p. Cambridge, UK.

López, C.M. 2014. Modelo sismo–tectónico esquemático de los principales sistemas de fallas en el sector del volcán Nevado del Ruiz y su relación con el sistema volcánico. Master thesis, Universidad de Caldas, 113 p. Manizales, Colombia.

Lucchi, F. 2013. Stratigraphic methodology for the geological mapping of volcanic areas: Insights from the Aeolian Archipelago (southern Italy). Geological Society of London, Memoirs 37, p. 37–53. London. https://doi.org/10.1144/M37.5

Martí, J., Groppelli, G. & Brum da Silveira, A. 2018. Volcanic stratigraphy: A review. Journal of Volcanology and Geothermal Research. 357: 68–91. https://doi.org/10.1016/j.jvolgeores.2018.04.006

Martínez, L.M., Valencia, L.G., Ceballos, J.A., Narváez, B.L., Pulgarín, B.A., Correa, A.N., Navarro, S, Murcia, H.F., Zuluaga, I., Rueda, J.B. & Pardo, N. 2014. Geología y estratigrafía del Complejo Volcánico Nevado del Ruiz. Servicio Geológico Colombiano, unpublished report, 853 p. Bogotá.

McCourt, W.J. 1984. The geology of the Central Cordillera in the Departments of Valle del Cauca, Quindío and NW Tolima (Sheets 243, 261, 262, 280 and 300). Ingeominas–Misión Británica, Internal report 1960, 54 p. Cali.

McCourt, W.J., Aspden, J.A. & Brook, M. 1984. New geological and geochronological data from the Colombian Andes: Continental growth by multiple accretion. Journal of the Geological Society, 141(5): 831–845. https://doi.org/10.1144/gsjgs.141.5.0831

McCourt, W.J., Mosquera, D., Nivia, Á. & Núñez, Á. 1985. Mapa geológico plancha 243 Armenia. Scale 1.100 000. Ingeominas. Bogotá.

Mosquera, D., Marín, P., Vesga, C. & González, H. 1998. Geología de la plancha 225 Nevado del Ruiz. Scale 1:100 000. Ingeominas. Bogota.

Nelson, W.H. 1962. Contribución al conocimiento de la cordillera Central de Colombia sección entre Ibagué y Armenia. Servicio Geológico Nacional, Boletín Geológico, 10(1–3): 161–202.

Neuwerth, R. 2009. Lithostratigraphical and tectono–sedimentary study of the Plio–Pleistocene infill of the Interandean North Cauca Valley Basin (Colombia). Doctoral thesis, Université de Genève, 157 p. Genève, Switzerland. https://doi.org/10.13097/archive-ouverte/unige:18948

Nivia, A. 2001. Geología del departamento del Valle del Cauca. Scale 1:250 000. Ingeominas. Bogotá.

Pardo, N., Pulgarín, B., Betancourt, V., Lucchi, F. & Valencia, L.J. 2019. Facing geological mapping at low–latitude volcanoes: The Doña Juana Volcanic Complex study–case, SW–Colombia. Journal of Volcanology and Geothermal Research, 385: 46–67. https://doi.org/10.1016/j.jvolgeores.2018.04.016

París, G., Machette, M.N., Dart, R.L. & Haller, K.M. 2000. Map and database of Quaternary faults and folds in Colombia and its offshore regions. U.S. Geological Survey, Open–File report 00–0284, 61 p. Denver, USA.

Pulgarín, B., Tamayo–Álzate, M., Valencia–Ramírez, L.G., Ceballos–Hernández, J.A., Correa–Tamayo, A.M., Cruz–Toro, Y.P. & Méndez–Fajury, R.A. 2017. Geología y estratigrafía del Complejo Volcánico Paramillo de Santa Rosa. Servicio Geológico Colombiano, unpublished report, 388 p. Bogotá.

Ramsey, C.B. 2013. OxCal 4.2 Manual. https://c14.arch.ox.ac.uk/oxcalhelp/hlp_contents.html (consulted in October 2016).

Reimer, P.J., Bard, E., Bayliss, A., Beck, J.W., Blackwell, P.G., Ramsey, C.B., Buck, C.E., Cheng, H., Lawrence, E., Friedrich, M., Grootes, P.M., Guilderson, T.P., Haflidason, H., Hajdas, I., Hatté, C., Heaton, T., Hoffmann, D.L., Hogg, A.G., Hughen, K.A., Kaiser, K.F., Kromer, B., Manning, S.W., Niu, M., Reimer, R.W., Richards, D.A., Scott, E.M., Southon, J.R., Staff, R.A., Turney, C.S.M. & van der Plicht, J. 2013. IntCal13 and Marine13 radiocarbon age calibration curves 0–50 000 years cal BP. Radiocarbon, 55(4): 1869–1887. https://doi.org/10.2458/azu_js_rc.55.16947

Restrepo, J.J. & Toussaint, J.F. 1976. Edades radiométricas de algunas rocas de Antioquia, Colombia. Publicación Especial Geológica, (6): 1–15. Medellín.

Restrepo, J.J. & Toussaint, J.F. 1985. Desarrollo mesocenozoico de los Andes noroccidentales de Colombia. VI Congreso Latinoamericano de Geología. Memoirs I, p. 95–96. Bogotá.

Robertson, K., Flórez, A. & Ceballos, J.L. 2002. Geomorfología volcánica, actividad reciente y clasificación en Colombia. Cuadernos de Geografía: Revista Colombiana de Geografía, 11(1–2): 37–76.

Salvador, A. 1994. International stratigraphic guide: A guide to stratigraphic classification, terminology, and procedure. 2nd edition. The International Union of Geological Sciences & The Geological, Society of America, 214 p. Boulder, USA. https://doi.org/10.1130/9780813774022

Schmid, R. 1981. Descriptive nomenclature and classification of pyroclastic deposits and fragments: Recommendations of the IUGS Subcommission on the Systematics of Igneous Rocks. Geology 9 (1) 41–43. https://doi.org/10.1130/0091-7613(1981)9<41:DNACOP>2.0.CO;2

Suter, F. 2008. Tectono–sedimentary study of the Interandean north Cauca Valley Basin, central western Colombia. Doctoral thesis, Université de Genève, 145 p. Genève. https://doi.org/10.13097/archive-ouverte/unige:2281

Taboada, A., Rivera, L.A., Fuenzalida, A., Cisternas, A., Philip, H., Bijwaard, H., Olaya, J. & Rivera, C. 2000. Geodynamics of the northern Andes: Subductions and intracontinental deformation (Colombia). Tectonics, 19(5): 787–813. https://doi.org/10.1029/2000TC900004

Thouret, J.C. 1988. La Cordillère Centrale des Andes de Colombie et ses bourdures: Morphogenèse Plio – Quaternaire et dynamique actuelle et recente d'une cordillère volcanique englacée. Doctorade thesis, Université Joseph Fourier, 327 p. Grenoble, France.

Thouret, J.C. & van der Hammen, T. 1981. Una secuencia holocénica y tardiglacial en la cordillera Central de Colombia: Aspectos geomorfológicos, pedológicos y paleoecológicos en el área del Parque Nacional de los Nevados, Tolima, Risaralda. Revista CIAF. 6 (1–3): 609–634. Bogotá.

Thouret, J.C., Murcia, L.A., Salinas, R. & Vatin–Pérignon, N. 1985. Cronoestratigrafía mediante dataciones K/Ar y ^{14}C de los volcanes compuestos del Complejo Ruiz–Tolima y aspectos volcano–estructurales del Nevado del Ruiz, cordillera Central, Colombia. VI Congreso Latinoamericano de Geología. Memoirs, p. 387–452. Bogotá.

Thouret, J.C., van der Hammen, T., Salomons, B. & Juvigné, E. 1997. Late Quaternary glacial states in the cordillera Central, Colombia, based on glacial geomorphology, tephra–soil stratigraphy, palynology, and radiocarbon dating. Journal of Quaternary Science, 12(5): 347–369.

Toro, G.E. & Hermelín, M. 1991. Tefraestratigrafía del departamento de Risaralda. Centro de Investigaciones de la Universidad Eafit, unpublished report, 134 p. Medellín, Colombia.

van der Hammen, T. 1960. Estratigrafía del Terciario y Maastrichtiano continentales y tectogénesis de los Andes colombianos. Boletín Geológico, 6(1–3): 67–128.

van der Hammen, T. 1985. The Plio–Pleistocene climatic record of the tropical Andes. Journal of the Geological Society, 142(3): 483–489. https://doi.org/10.1144/gsjgs.142.3.0483

Walker, G.P.L. 1973. Explosive volcanic eruptions: A new classification scheme. Geologische Rundschau, 62(2): 431–446.

Explanation of Acronyms, Abbreviations, and Symbols:

AMS	Accelerator mass spectrometry
Caltech	California Institute of Technology
DEM	Digital elevation model
ICP–MS	Inductively coupled plasma mass spectrometry
JPL	Jet Propulsion Laboratory
NASA	National Aeronautics and Space Administration
PDCs	Pyroclastic density currents
PQV	Paramillo del Quindío Volcano
Pre–PSRV	Pre–Paramillo de Santa Rosa Volcano
PSRV	Paramillo de Santa Rosa Volcano
PSRVC	Paramillo de Santa Rosa Volcanic Complex
UAVSAR	Uninhabited aerial vehicle synthetic aperture radar
XRF	X–ray fluorescence
y BP	Years before present

Authors' Biographical Notes

Bernardo Alonso PULGARÍN–ALZATE is a geologist engineer (1987) with an MS in volcanology (2000) from the Universidad Nacional Autónoma de México. His professional job has been focused on understanding volcanic geology–stratigraphy and the eruptive histories of volcanoes as well as in the searching for good practices for standardization of volcanoes geological maps. He also has experience working with volcanic hazards, glacier retreat, and socialization and communication with communities that live under threat of geological hazards. He has worked for the Servicio Geológico Colombiano (SGC) at the Observatorio Vulcanológico y Sismológico de Popayán for 32 years. He has carried out geological work and research on several Colombian volcanoes (Puracé, Los Coconucos volcanic chain, Nevado de Santa Isabel, Nevado del Huila, Doña Juana, Sotará, Sucubún, Nevado del Ruiz, Paramillo de Santa Rosa, and Galeras). He is currently the coordinator of the Grupo de Geología de Volcanes of the SGC.

Mauricio TAMAYO–ALZATE is a geologist and has a master's degree in geographic information technologies. He has worked at the Servicio Geológico Colombiano since 2014, where he has conducted research activities in geology, stratigraphy, cartography, and eruptive volcanic history. He is part of the Grupo de Geología de Volcanes of the Servicio Geológico Colombiano, where he studies volcanoes such as Paramillo de Santa Rosa and Galeras and the geology of the Quindío–Risaralda Fan. He is interested in geological mapping, stratigraphy, volcanic cartographic standards, and GIS.

Ana María CORREA–TAMAYO is a geologist (1992) with a PhD in geology (2009) from the Universidad Complutense de Madrid. Her professional job has been focused on volcanic cartography and stratigraphy, petrographic and geochemical studies of volcanoes, and their eruptive history. She has been working at the Servicio Geológico Colombiano (SGC) for 10 years. She has performed geological work and research on several Colombian volcanoes (Nevado del Huila, Azufral, Paramillo de Santa Rosa, Doña Juana, Nevado del Ruiz, and Sotará). She is currently a member of the Grupo de Geología de Volcanes of the SGC.

Julián Andrés CEBALLOS–HERNÁNDEZ is a geologist who graduated from the Universidad de Caldas (2007) and has worked at the Observatorio Vulcanológico y Sismológico de Manizales of the Servicio Geológico Colombiano since 2012. He was the technical coordinator for the "Volcanic Hazard Map of NRV, Third Version". He has participated in geological mapping and research in the Nevado del Ruiz, Paramillo de Santa Rosa, and Galeras Volcanic Complexes and has worked with computational simulations of lahars from the Nevado del Ruiz, Galeras, Chiles, and Cerro Negro Volcanoes. He also has experience working on socialization–communication projects within the framework of volcanic risk management.

Yeni Patricia CRUZ–TORO is a geologist who has worked at the Servicio Geológico Colombiano since 2013, and her first supporting activities in the petrographic microscope laboratory consisted of organizing all the available material from the thin section collection of the Servicio Geológico Colombiano. Since 2015, she has been part of the Grupo de Geología de Volcanes of the Servicio Geológico Colombiano, involved in researching volcanoes such as Paramillo de Santa Rosa and Galeras and performing research in geology, petrography, cartography, and eruptive volcanic history.

Ricardo MÉNDEZ–FAJURY is a geologist engineer of the Universidad Nacional de Colombia (1985) with a specialization in docencia universitaria at the Universidad Católica de Manizales. He has been working for the Servicio Geológico Colombiano in the Observatorio Vulcanológico y Sismológico de Manizales for 32 years in the areas of volcanic geology and geochemistry and the socialization and communication of information related to geological origins, geoarchaeology, and historical collections of volcanic activity. He has carried out geological work and research on several Colombian volcanoes (Nevado del Ruiz, Nevado Santa Isabel, Nevado del Huila, Cumbal, Cerro Machín, and Paramillo de Santa Rosa).